8-2016

# Fabrication and Characterization of a Novel Porous Polymer Microsphere - Hydrogel Composite for Cell Therapy

Prathik Thulluri
*Clemson University*

# FABRICATION AND CHARACTERIZATION OF A NOVEL POROUS POLYMER MICROSPHERE - HYDROGEL COMPOSITE FOR CELL THERAPY

---

A Thesis
Presented to
the Graduate School of
Clemson University

---

In Partial Fulfillment
of the Requirements for the Degree
Master of Science
Bioengineering

---

by
Prathik Thulluri
August 2016

---

Accepted by:
Dr. Ken Webb, Committee Chair
Dr. Scott Taylor
Dr. Jiro Nagatomi

# ABSTRACT

For patients with organ failure complications, organ transplantation is not always an option due to a shortage of donors along with obstacles such as risk of pathogen transfer and the possibility of immune rejection. Tissue engineering approaches based on cell therapy provide a promising alternative that could potentially solve these problems. The success of cell therapy for tissue repair and regeneration requires reliable and efficient cell delivery methods. Currently, hydrogels are favored matrices for cell delivery because of their ability to be injected by minimally invasive techniques as viscous liquids and crosslinked *in situ* under mild conditions compatible with the homogeneous incorporation of cells and bioactive molecules. However, hydrogels have several limitations including relatively weak mechanical properties that limit cell proliferation and allow premature contraction, as well as their hydrophilic composition that offers little capacity for binding secreted extracellular matrix (ECM) molecules to support higher order assembly. The long-term objective of this research is to develop a composite cell delivery matrix composed of a biosynthetic hydrogel containing porous, hydrophobic microparticles. Toward this end, the project examined optimization of processing variables to create porous Strataprene® 3534 polymer microspheres, examined their concentration-dependent effects on hydrogel physicochemical properties, and evaluated their ability to support cell adhesion. By decreasing polymer and increasing porogen concentrations, particles with increased porosity were attained. Hydrogel/particle composites maintained mechanical integrity with modest decreases in gelation efficiency and elastic modulus relative to hydrogel-only controls. Strataprene®

3534 polymer films supported robust cell adhesion and spreading approximating tissue culture plastic controls and substantially greater than poly (lactide-co-glycolide) films. Cell adhesion to microparticles was less efficient, perhaps due to entrapment of poly(vinyl alcohol) used to stabilize the secondary emulsion on the surface of the microparticles. Overall, these studies demonstrate that highly porous polymer microparticles can be achieved and successfully incorporated into hydrogels to create composites without substantially altering the gel's physical properties. Future studies will examine improvement of cell adhesion and composite functionality for enhancing cell proliferation and ECM accumulation.

# DEDICATION

I would like to dedicate this thesis to my parents for their unconditional love and support. You're the reason I'm 6'3" and for that, I am eternally grateful.

# ACKNOWLEDGMENTS

I would like to thank my research advisor Dr. Ken Webb for his guidance and mentorship over the course of this project. I would also like to thank my committee members Dr. M. Scott Taylor, Dr. Jiro Nagatomi and Dr. Jeoung Soo Lee for their support of this project. I would like to thank the current and former members of the MicroEnvironmental Engineering laboratory especially Sooneon Bae, Zachary Reinhardt and Ho-Joon Lee for their contributions to this research. Additionally, I would like to thank Dr. Guzeliya Korneva for her assistance with spin coating, Dr. Taghi Darroudi and George Wetzel for their training on scanning electron microscopy.

TABLE OF CONTENTS

Page

TITLE PAGE ..... i

ABSTRACT ..... ii

DEDICATION ..... iv

ACKNOWLEDGMENTS ..... v

LIST OF TABLES ..... viii

LIST OF FIGURES ..... ix

CHAPTER

I. INTRODUCTION AND BACKGROUND ..... 1

1.1 Advent of Tissue Engineering ..... 1
1.2 Scaffold based Tissue Engineering ..... 2
1.3 Current microscale approaches in cell therapy ..... 4
1.4 Effect of substrate stiffness on cell proliferation ..... 9
1.5 ECM and its role in tissue development ..... 11

II. OBJECTIVES ..... 16

2.1 Project Rationale and Hypothesis ..... 16
2.2 Aims ..... 19

III. MATERIALS AND METHODS ..... 20

3.1 Materials ..... 20
3.2 Fabrication of porous polymer microspheres ..... 21
3.2.1 Double emulsion solvent evaporation method ..... 21
3.2.2 Scanning Electron Microscopy ..... 23
3.2.3 Preparation of uniform microsphere suspensions ..... 23
3.3 Hydrogel preparation ..... 24
3.3.1 Preparation of degradable, crosslinkable PEG diacrylate macromers ..... 24
3.3.2 Synthesis of PEG-bis-(2-chloropropanoate) ..... 25
3.3.3 Hydrogel photopolymerization ..... 27

Table of Contents (Continued)

Page

3.3.4 Gel content and swelling behavior ..... 27
3.3.5 Uniaxial tensile testing ..... 28
3.3.6 Statistical analysis ..... 29
3.4 Cell adhesion studies ..... 29
3.4.1 Cell culture ..... 29
3.4.2 Cell adhesion on spin coated glass slides ..... 30
3.4.3 Cell seeding experiment ..... 30

IV. RESULTS AND DISCUSSION ..... 32

4.1 Double emulsion solvent evaporation ..... 32
4.1.1 Optimization of process variables ..... 32
4.1.2 Statistical analysis of baseline and optimized Strataprene® microspheres ..... 38
4.1.3 Preparation of uniform microsphere suspensions ..... 38
4.2.1 Synthesis and characterization of PEG-bis-(AP) ..... 40
4.2.2 Gel content and swelling behavior ..... 42
4.2.3 Uniaxial tensile test ..... 43
4.3.1 Cell adhesion on spin coated glass slides ..... 44
4.3.2 Static cell seeding ..... 46

V. CONCLUSIONS AND FUTURE STUDIES ..... 47
5.1 Conclusions ..... 47
5.2 Future studies ..... 48

REFERENCES ..... 50

LIST OF TABLES


| Table | | Page |
|---|---|---|
| 1.1 | Conventional fabrication techniques and corresponding porosity | 5 |
| 3.1 | Variation of process variables | 22 |
| 4.1 | Pore sizes and Diameters of baseline and optimized microspheres | 38 |
| 4.2 | Gel and equilibrium water content at different particle concentrations | 42 |

LIST OF FIGURES


| Figure | | Page |
|---|---|---|
| 1.1 | Gap between number of donors and patients on waiting list | 1 |
| 1.2 | Overview of scaffold based tissue engineering approach | 3 |
| 1.3 | Effects of matrix mechanics on cell behavior | 10 |
| 1.4 | Schematic representation of assembly of collagen I | 12 |
| 3.1 | Illustration of double emulsion solvent evaporation | 21 |
| 3.2 | Preparation of degradable PEG-bis-acrylate macromers | 25 |
| 4.1 | Baseline porous PLGA microspheres | 33 |
| 4.2 | Montage of microsphere batches with varied parameters | 34 |
| 4.3 | Batch 5 microspheres with optimized parameters | 36 |
| 4.4 | Freeze dried microspheres in 1X PBS | 39 |
| 4.5 | Non-freeze dried microspheres in 1X PBS | 39 |
| 4.6 | Non-freeze dried microspheres with 0.36% HA in 1X PBS | 40 |
| 4.7 | Structure and $_1$H-NMR spectrum of PEG-bis-(2-CP) | 41 |
| 4.8 | Elastic moduli of PEGDA/HA hydrogels loaded with varying concentrations of microspheres | 43 |
| 4.9 | Fluorescent images of rat fibroblasts on TCP | 44 |
| 4.10 | Fluorescent images of rat fibroblasts on PLGA microspheres in same and separate wells | 45 |
| 4.11 | Fluorescent images of rat fibroblasts on Strataprene® spin coated films | 45 |

List of Figures (Continued)

Page

4.12 Fluorescent images of rat fibroblasts on Strataprene® microspheres in same and separate wells.....46

# CHAPTER ONE

# INTRODUCTION AND BACKGROUND

## 1.1 Advent of Tissue Engineering

For a long time, organ transplantation was thought of as the only solution for most end stage organ failure based complications. The efficacy of this mode of treatment however was severely limited due to the ever widening gap between the number of prospective organ donors and patients placed on the organ transplant waiting list. In the United States, at the end of the year 2013 for example, there were 121,272 patients waiting for transplantation, while only 28,954 transplants were performed and organs from 14,257 donors were recovered [1].

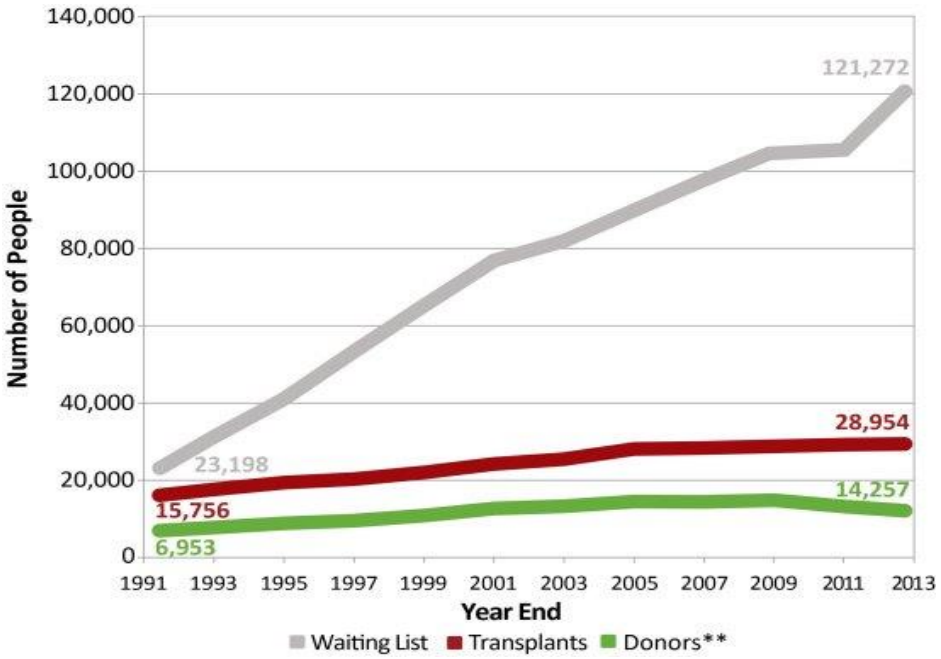


**Figure 1.1: Gap between number of donors and patients on waiting list [1]**

The reality as evidenced by **Figure 1.1** is that the number of candidates waiting will continue to dwarf the number of donor organs available. There are also difficulties

such as the risk of pathogen transfer, possibility of immune rejection and steep costs associated with organ transplantation. This led to the birth of tissue engineering based approaches as an alternative method to address the limitations of organ transplantation.

Tissue engineering is an interdisciplinary field that applies the principles of engineering and life sciences towards the development of biological substitutes that restore, maintain or improve tissue function (Langer and Vacanti 1993) [2]. This approach adopts three general strategies for the creation of new tissue [2] [3]. The first strategy involves the use of isolated cells from the patient or designing cell substitutes to perform specific function before infusion into the patient [2]. The second strategy involves the use of tissue inducing substances such as growth factors and the development of methods to deliver these molecules to their targets [2]. The third approach relies on cells being placed on or within matrices or scaffolds which act as a membrane to isolate the cells from the body while allowing permeation of nutrients and wastes. Such scaffolds are traditionally fashioned from natural material such as collagen or from synthetic polymers [2]. The success of tissue engineering depends on understanding tissue behaviors such as function and regeneration.

**1.2 Scaffold based Tissue Engineering**

For this project, we use a variant of the scaffold based cell therapy approach (first strategy) defined by Langer and Vacanti. This method involves a combination of viable cells, biomolecules and a structural scaffold which supports cell migration, growth and differentiation and guides tissue development and organization into a mature and healthy state [4].

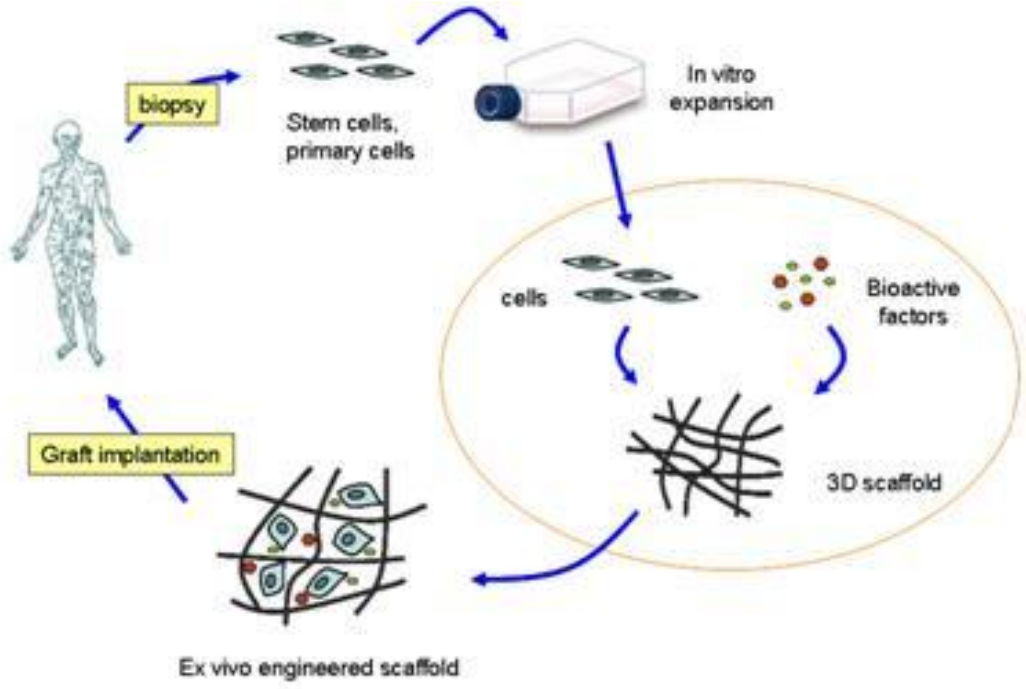


**Figure 1.2: Overview of scaffold based tissue engineering approach [9]**

In theory, scaffolds in tissue engineering applications will have to meet certain minimum requirements for biochemical chemical and physical properties in order to fulfil their function. They must provide sufficient initial mechanical strength and stiffness to substitute for the mechanical function of the diseased or damaged tissue [4]. They need to maintain structural integrity during the growth and remodeling process [4] Scaffold architecture must allow for initial cell attachment, migration, mass transfer of nutrients and metabolites, and space for development and remodeling of tissue [4]. The degradation and resorption kinetics of the scaffold need to be tuned to the rate of tissue

development [4]. Ideally, as the scaffold is degraded, the cells will deposit their own extracellular matrix molecules that will eventually form three dimensional structures that closely mimic the native tissue architecture [5].

Some commonly used cell delivery systems for cell therapy at present include injectable porous polymeric microspheres and cell laden hydrogels. Injectable cell delivery methods are preferred to implantable methods as they would not require surgery and are minimally invasive [6] [5].

### 1.3 Current microscale approaches in cell therapy

Porous polymeric scaffolds are extensively used in regenerative medicine (especially PLGA based) because they permit sufficient cell adhesion and survival. Also, PLGA is preferred because in certain applications it has already been FDA approved and has tunable degradation kinetics so as to match the rate of cell growth [5]. In order to promote tissue repair, scaffolds need to be mechanically stiff enough to promote cell proliferation and shielding of the cells from stresses experienced by the system in vivo during and after injection [7]. They must also have suitable mechanical properties and adequate porosity and pore diameter to support cell spreading, proliferation and migration in addition to nutrient delivery, waste removal and vascularization.

It has been demonstrated in literature that both micro (<50 μm) and macro-porosity (> 50 μm) is essential to influence tissue and cell function. If pores are too small cells can’t migrate in towards the center of the construct limiting the diffusion of nutrients and removal of waste products. Conversely, if pores are too large there is a decrease in specific surface area available limiting cell attachment [8]. Micropores

provide greater surface area for better cell adhesion, while macropores provide a larger void space for tissue regeneration in vivo when compared to non-porous PLGA microspheres [8]. Studies have shown that the ideal pore size is 3-5 times the size of the protein or cell they carry [8]. However, based on the application a balance must be found as increasing the porosity of a scaffold causes a decrease in mechanical properties [5].

Porous polymeric scaffolds can be fabricated using a multitude of ways. Table 1.1 provides a brief overview of some conventional fabrication techniques along with the corresponding pore size and porosity induced [4].

**Table 1.1: Conventional fabrication techniques and corresponding porosity**

| Technique | Porosity (%) | Pore size (μm) | Material used |
|---|---|---|---|
| Gas foaming | <80 | <350 | PLLA |
| Solvent casting particulate leaching | 82 - 92 | <200 | PLA, PLGA, PVA |
| emulsion solvent evaporation | <80 | <10 | PLGA, PLA |

Gas foaming method is based on inducing the formation of inert gas such as $CO_2$ within a precursor solution. The formed gas transforms the liquid into a foam entity. This foam can be stabilized by freezing the liquid phase with subsequent lyophilization. Solvent casting particulate leaching involves dissolving a polymer in an organic solvent along with sieved salt particles (sodium chloride). The solvent is then extracted by vacuum treatment followed by leaching out of salt particles by immersion in DI water. This method can be used to fabricate 2D scaffolds only a few mm thick. However,

neither of these methods allow for achievement of microporosity. The double emulsion solvent evaporation method however can be modified to obtain pore sizes in a wide range and can be used to fabricate microscaffolds for cell therapy. The double emulsion solvent evaporation method was used in this study to make porous polymeric microspheres. Briefly, micro-scaffolds were fabricated using a water/oil/water double emulsion solvent evaporation method using ammonium bicarbonate as a porogen. In this technique a small aqueous phase (porogen in deionized water) is first emulsified within a polymer solvent phase. This emulsion is re-emulsified in a large volume of aqueous phase to generate a water in oil in water (W/O/W) double emulsion. The volatile solvent is removed as it diffuses into the aqueous medium and evaporates at the air water interface. As the solvent evaporates, the PLGA based microspheres are precipitated and collected by centrifugation [8].

Once the scaffolds with required size, porosity and pore diameter are fabricated by the suitable technique, the cells are loaded onto the scaffolds, and their viability, in vitro is determined before injection into the target site in a particular animal model to observe potential therapeutic effects.

The other major cell delivery system utilizes hydrogels for tissue engineering. Hydrogels have long received attention as matrices for therapeutic cell transplantation based on their ability to be delivered using minimally invasive methods and crosslinked in situ under mild conditions [10]. They are also structurally and compositionally similar to extracellular matrix and can provide viscoelastic mechanical properties similar to many soft tissues.

Hydrogels for tissue engineering applications are generally prepared from either naturally derived or synthetic macromolecules. Hydrogels formed from naturally derived materials generally exhibit good cell adhesion and cell mediated enzymatic degradation, but end up lacking in terms of mechanical properties. They can end up undergoing rapid degradation unless stabilized by crosslinking agents. At the same time, hydrogels prepared from synthetic materials such as polyethylene glycol (PEG) allow for improved network physical and chemical properties but do not possess the bioactivity to support proper cell adhesion and cell mediated degradation [10]

One commonly used approach to overcome this drawback associated with hydrogels has been the modification of synthetic networks with oligopeptides derived from natural ECM to support cell adhesion (e.g. RGD) and cell mediated degradation (e.g. MMP). Although, this method has found some success there are certain difficulties associated with the synthesis of oligopeptides, their reduced degradation kinetics and a tradeoff between bioactivity and mechanical properties during gel formulation [10].

An alternative approach involves the use of modified naturally derived macromolecules to form hybrid hydrogels which could potentially support higher rates of enzymatic degradation and better bioactivity and cell adhesion. It has been previously shown by our lab [10] semi-interpenetrating polymer networks (interlaced on a polymer scale without being covalently bonded) comprised of PEGDA and native HA show increased cell spreading and proliferation compared to synthetic networks as well as increased susceptibility to cell mediated enzymatic degradation due to the creation of HA enriched microdomains during the semi-IPN polymerization. These gels however, have

limited ECM binding properties due to the hydrophilicity of PEG, which is discussed in detail in Chapter 2.

For this research study, the advantageous features of the PEGDA/HA semi-IPN and porous polymer microspheres were combined to provide improved cell therapy

The therapeutic benefits of such scaffold based cell delivery systems however, is severely limited due to cell loss and cell death. Mechanical damage during injection, high leakage to surrounding tissues, improper vascularization and inflammation in the *in vivo* microenvironment could all contribute to poor cell retention and viability [7]. The lack of reliable cell delivery methods is one of the main problems that are preventing tissue engineering from realizing its true potential and showing significant clinical results.

Traditional hydrogel or porous polymer microsphere based tissue engineering approaches also have limitations to their efficacy. Hydrogels are mechanically weak substrates which limit proper cellular spreading on the substrate, inhibiting subsequent proliferation and tissue development.

At the same time polymeric microspheres are not as efficient as hydrogels for incorporation of cells. Their efficacy is also limited due to cell loss and cell death due to insufficient shielding from the stresses during injection and in the dynamic *in-vivo* environment.

In this study a novel hydrogel – porous polymer microsphere composite was developed that overcomes these drawbacks by using the hydrogel as a carrier for the cells and for stress shielding to maintain cell viability, while the porous polymeric

microspheres suspended within the hydrogel provide a substrate with suitable mechanical properties for improved cell proliferation.

Before the composite is discussed in detail, it is important to understand the effect of substrate mechanical properties on cell proliferation and the role of extracellular matrix in tissue development to better appreciate the functioning of our cell delivery system.

### 1.4 Effect of substrate stiffness on cell proliferation

Most normal tissue cells are not viable when suspended in a fluid and are said to be anchorage dependent. These cells must adhere to a solid substrate in order to activate phenotypic functions for biological processes such as tissue cohesion, repair and proliferation.

Cells adhere to solid substrates that range in stiffness from soft to rigid and that also vary in topography and thickness. The stiffness of the substrate to which cells adhere can have a profound effect on cell structure and protein expression which has important implications for tissue development and regeneration [11]. At the cellular scale, normal tissue cells probe substrate elasticity as they anchor and pull on their surroundings. As a cell adheres to the substrate through focal adhesions, it pulls on the substrate via its actin-myosin cytoskeleton, senses resistance, and in turn responds to this resistance through the cytoskeleton [12]. Such processes are dependent in part on myosin based contractility and transcellular adhesions centered on integrins, cadherins and other adhesive molecules to transmit forces to substrates [12] [13].

Substrate stiffness has many effects on cell function. At the basic level, stiffness can regulate cell growth, viability and resistance to apoptosis. Fibroblast cell lines, for instance, undergo more apoptosis and less proliferation on soft as opposed to stiff substrates [12]. Stiffness can also regulate differentiation state, lineage commitment and the degree of cell matrix adhesion. The mechanical properties of the substrate to which cells adhere influences gene expression and post translational modifications at the most basic level [12].

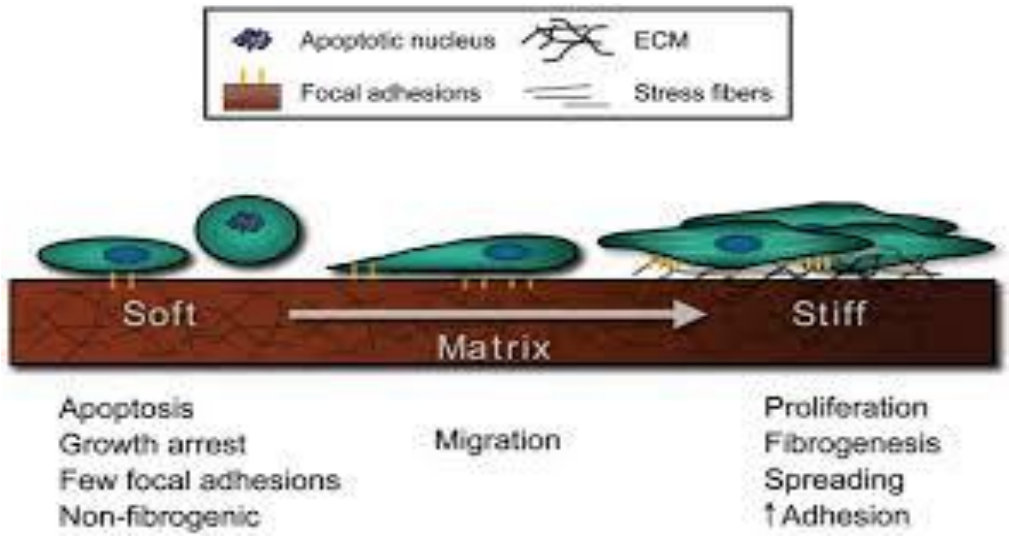


**Figure 1.3: Effects of matrix mechanics on cell behavior [12]**

As shown in Figure 1.3, soft substrates (like lightly cross linked hydrogels) show diffuse and dynamic adhesion complexes in contrast to stiff substrates which show cell adhesion with stable focal adhesions. The cells adhering on soft materials probe substrate elasticity by pulling on the material. When they don't sense sufficient resistance it can lead to substrate buckling. There are few focal adhesions in this case which limits the strength of cellular adhesion. As softer substrates don't provide much resistance to the

actin myosin cytoskeleton, the cells exhibit a relatively round morphology. The cells adhering to stiff materials however, experience resistance when their actin myosin cytoskeleton pulls on the substrate. This leads to cytoskeletal changes causing a more spread morphology, which in turn activates cell proliferation.

Consistent with a role for signaling in stiffness sensing, tyrosine phosphorylation on multiple proteins (including paxillin) appears greatly enhanced in cells on stiffer substrates, whereas nonspecific hyperphosphorylation drives focal adhesion formation on soft materials [14]. Inhibition of actomyosin contractions, in contrast, largely eliminates prominent focal adhesions, whereas stimulation of contractility drives integrin aggregation into adhesions [14]

The tactile sensing of substrate stiffness feeds back on cell adhesion, morphology and on net contractile forces. Cells on soft substrates are less contractile than on stiff substrates, which lead to their adhesion strength being lower as well [14].

Thus, substrate stiffness which influences strength of cell adhesion to its extracellular environment is a crucial factor in any tissue engineering strategy as the strength of cell adhesion determines the maintenance of cell viability, rate of cell proliferation and in turn tissue development.

**1.5 ECM and its role in tissue development**

The extracellular matrix represents the secreted product of resident cells within each tissue and organ and is made up of a mixture of structural and functional proteins arranged in a unique tissue specific three dimensional ultrastructure [4]. These molecules (mostly proteins) provide the mechanical strength required for proper tissue function and

act as a signaling mechanism between adjacent cells and between the cells and itself [4]. Most of the extracellular matrix molecules are well recognized and they form a complex mixture of proteins, glycosaminoglycans, glycoproteins and small molecules arranged in a tissue specific architecture.

Collagen is the most abundant protein within the mammalian ECM constituting greater than 90% of its dry weight [4] [15]. More than 20 distinct types of collagen have been identified, each with a specific biologic function. Type I collagen (abundant in tendinous and ligamentous structures) for example, provide necessary strength to support the uniaxial and multiaxial mechanical loading to which these tissues are routinely subjected [15].

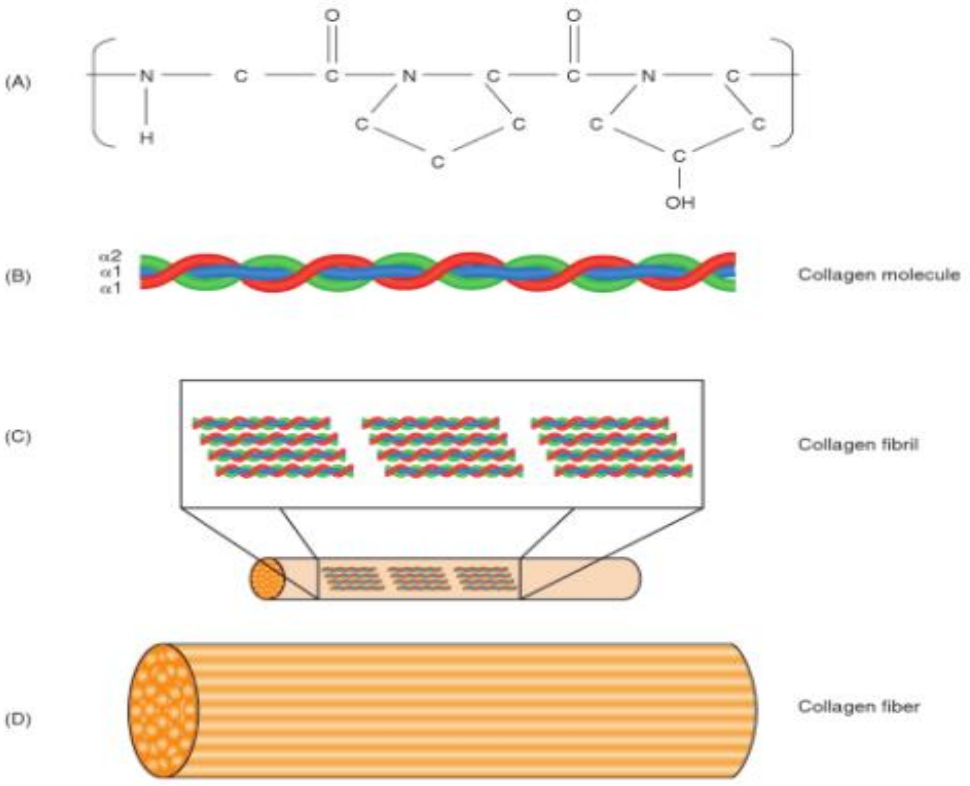


**Figure 1.4: Schematic representation of assembly of collagen I [4]**

In the above figure (A) represents individual polypeptide chains consisting of repeating sequence Gly – X – Y (X, Y are often proline and hydroxiproline respectively), (B) Collagen is made up of three polypeptide strands which are left handed helixes, (C) Collagen molecules self-assemble into collagen fibrils, (D) Collagen fibers formed assembly of collagen fibrils [4].

Other major components of ECM include fibronectin, which is second only to collagen in terms of quantity within the extracellular matrix and is a dimeric molecule that serves as a ligand for adhesion of many cell types [4]. Laminin is another complex adhesion protein found in the ECM and plays and important role in early embryonic development [4]. Glycosaminoglycans are another component of the extracellular matrix that bind growth factors and cytokines (through heparin mediated binding), promote water retention and contribute to the gel properties of the ECM [4]. ECM also contains cytokines and growth factors (vascular endothelial growth factor, fibroblast growth factor etc.) in small quantities, which act as potential modulators of cell behavior.

The ECM plays an intrusive role in cellular activities and can affect cellular behavior [16]. For example, the controlled interaction of cells with specific ECM architectures is critical to maintain cell phenotype [17]. The cell surface contains receptors capable of responding to extracellular signals. As soon as a ligand receptor interaction is established, the biochemical machinery involved in the control of gene expression starts [16].

Cell adhesion is crucial for tissue formation and integrity. It is essential to know how cells interact with ECM and transduce extracellular stimuli into an intracellular

event to better understand tissue engineering strategies [18]. The identification of cell binding sites with extracellular molecules is a key step in studying cell – ECM interactions.

The cell surface possesses non integrin and integrin receptors. Non integrin receptors consist of proteoglycans, CD36, and some laminin binding proteins. The most crucial receptors in cell binding however are the surface proteoglycans syndecan and CD44. Syndecan, in addition to binding collagens, fibronectin and thrombospondin binds bFGF (basic fibroblast growth factor). Syndecan is unique in the sense that it can co-localize both ECM molecules and growth factors to the cell surface and assemble signaling complexes with other receptors [16]. CD44 plays a vital role in cell adhesion and movement by binding type I and IV collagens and hyaluronan [16].

Integrins represent a large group of glycoprotein cell surface receptors [19]. When ECM molecules bind to a specific integrin receptor, a change in cytoplasmic domain of the receptor occurs associating the cytoskeleton at focal adhesion sites [19, 20]. This leads to an assembly of focal contact proteins with intracellular components such as phosphorylated proteins [20]. These changes can promote cytoskeletal rearrangement, which may alter the interactions of chromatin and nuclear matrix at the nuclear level [16]. This dynamic association of integrin receptors with actin cytoskeleton may also induce changes in cell shape, altering the ability of the cells to proliferate or differentiate [16].

There are two main ways in which the extracellular matrix can influence cell behavior. One of these is through cell – ECM interactions which may directly regulate cell functions through receptor mediated signaling [16] [18]. It has been shown in

literature that the molecules able to regulate cell adhesion can modulate the cellular response to other extracellular stimuli [21]. These ECM molecules may selectively stimulate specific types of signal transduction pathways that may affect cell proliferation and differentiation as a downstream effect. The second way in which the extracellular matrix may affect cell function is by mobilizing growth or differentiation factors on the cell surface (ECM – growth factor interactions), thus modulating cell proliferation and cell phenotype [16].

Thus, the extracellular matrix molecules play a crucial role in cell adhesion, proliferation, and tissue development and can be thought of as one of the main indicators of the efficacy of scaffold based cell therapy. The more extracellular matrix deposition and accumulation there is on a scaffold, the higher will be the rate of tissue regeneration.

# CHAPTER TWO

# OBJECTIVES

## 2.1 Project Rationale and Hypothesis

As mentioned in previous chapters, semi-interpenetrating polymer networks comprised of polyethylene glycol diacrylate (PEGDA) and native hyaluronic acid (HA), show increased cell spreading and proliferation compared to synthetic networks as well as increased susceptibility to cell mediated enzymatic degradation due to the creation of HA enriched microdomains during the semi-IPN polymerization. Despite the success of this approach, there are still limitations to cell therapy due to the protein repelling properties of PEG.

The inertness of PEG towards protein adsorption is due to its hydrophilicity, chain mobility and lack of ionic charge. The PEG backbone is mostly hydrogen bonded to water molecules that form a partially structured hydration layer. Adsorption of protein molecules requires the disruption of this layer. Protein adsorption also leads to the compression of the PEG layer which is entropically unfavorable. These features have led to several groups using PEG as a modifier to create a biocompatible but cell repelling surface. Thus, PEG based hydrogels used for cell therapy do not provide adequate capture of extracellular matrix proteins to allow for higher order assembly which is a crucial step in cell proliferation and subsequent tissue regeneration [22] [23] [24].

Hydrogels also possess relatively weak mechanical properties, which leads to cells forming diffuse and dynamic focal adhesions with low strength on the hydrogel

surface. This limits the extent of cytoskeletal rearrangement (cell spreading on substrate), and the rate of cell proliferation necessary to ensure efficient cell therapy.

Porous microspheres provide certain benefits by virtue of their mechanical properties. These particles are generally stiffer than hydrogels and cells form stable focal adhesions on their surface with spread morphology. This leads to higher rates of cell proliferation when compared to hydrogels. PLGA based microparticles can also effectively bind ECM molecules secreted by cells by virtue of their hydrophobicity. It was hypothesized that the benefits afforded by porous microparticles can be maximized by using a novel Strataprene® 3534 polymer synthesized by Poly-Med, Inc. due to its suitability for the cell scaffold application. Some key features of this polymer we are looking to exploit include:

1) It is a copolymer with repeat units with significantly more compliant than lactide and glycolide monomers, so it has improved mechanical properties when compared to traditionally used PLGA.

2) The degradation byproducts are less acidic than most traditionally used polymers, thereby improving the environment for cell growth.

3) The polymer by virtue of its structural differences compared to PLGA promotes better cellular attachment.

Based on the properties of porous microspheres, it was hypothesized that adding porous Strataprene® 3534 polymer microspheres to hydrogels would overcome the limitations associated with gels by:

1) improving mechanical properties at the micro level in the hydrogel enabling better cell proliferation.

2) providing hydrophobic domains able to bind and effectively capture extracellular matrix, thereby enhancing matrix accumulation and tissue growth.

The long term objective of this proposed research was to develop a hydrogel – porous polymer microsphere composite system for efficient cell therapy. First, porous Strataprene® polymer microspheres will be fabricated using a double emulsion solvent evaporation method with ammonium bicarbonate as a porogen [25]. The process variables will be optimized until the microspheres are characterized to have the appropriate diameter, pore size and porosity for our application by using scanning electron microscope [25] [26].

Next, a Polyethylene glycol diacrylate (PEGDA) macromere blend of PEG-bis-(acryloyloxy aceteate), PEG-bis-(acryloyloxy proponoate) and PEG-bis-(acryloyloxy butyrate) with hyarulonic acid and varying concentrations of porous polymeric microspheres was photopolymerized under a low intensity UV lamp to create the composites [27]. These composites with varying concentrations of microparticles were then mechanically characterized and their elastic moduli and gelation efficiencies were compared with hydrogel only controls.

Finally, cell adhesion properties of Strataprene® 3534 polymer films were compared with tissue culture plastic and poly (lactide-co-glycolide) (PLGA) controls followed by the evaluation of cell adhesion properties of the porous polymer microsphere component of our composite system.

Specifically, the composite was fabricated and its efficacy for cell therapy was evaluated using three aims:

**2.2 Aims**

**Aim 1:** Fabricate and characterize Porous Strataprene® 3354 polymer microspheres with appropriate diameter, pore size and porosity.

**Aim 2:** Develop and mechanically characterize a photo crosslinked hydrogel made from a PEGDA macromer blend.

**Aim 3:** Test cell adhesion properties of the polymer microsphere - hydrogel composite system in vitro.

.

# CHAPTER THREE

# MATERIALS AND METHODS

## 3.1 Materials

Strataprene® 3534 polymer (35/34/17/14 Caprolactone/L-Lactide/Glycolide/Trimethylene Carbonate Polyaxial Block, Random Copolymer) ($M_w$ 165±5 kDa) was generously donated by Poly-Med Inc. (Anderson, SC). Poly (lactic-co-glycolic acid) (PLGA) (74:26, I.V. 0.90 dl/g) was contributed by Purac BU Biomaterials (Gorinchem, Netherlands). Poly vinyl alcohol, Dichloromethane (HPLC grade), anhydrous dimethylformamide (DMF) and sodium bicarbonate were obtained from Acros organics (NJ, USA). Polyethylene glycol (PEG) was purchased from Fluka (Buchs, Switzerland). 2-chloropropionyl chloride, trimethylamine, sodium acrylate, 4-methoxyphenol, were purchased from Sigma-Aldrich (St Louis MO, USA). Ethyl ether, sodium sulfate and ammonium bicarbonate were purchased from Fisher Scientific (NJ, USA). Irgacure 2959 9@-hydroxy-1-{4-(hydroxyethoxy) phenyl]-2-methyl—propanone, I-2959) was purchased from Ciba® Specialty Chemicals (Basel, Switzerland). A dog bone shaped mold for photopolymerization of hydrogel for tensile testing was 3-D printed using KLIC-N-PRINT 3D printer**.**

Alexa Fluor® 594 phalloidin molecular probe was purchased from Life Technologies (OR, USA). Fluorescein diacetate was purchased from Thermo Fisher Scientific (OR, USA). All other materials were used as received.

### 3.2 Fabrication of porous polymer microspheres

Porous Strataprene® 3534 polymer and PLGA control microspheres were fabricated using a double emulsion solvent evaporation method. The process variables were optimized until the microspheres were characterized to have the appropriate diameter, porosity and pore size using scanning electron microscope.

#### 3.2.1 Double emulsion solvent evaporation method

Porous microspheres were created using a water in oil in water double emulsion method as shown in Figure 3.1. In the baseline fabrication process, 500 mg of ammonium bicarbonate (porogen) was dissolved in 2.5 ml deionized water. This water phase was then added to a solution of 500 mg of Strataprene® in 8 ml of dichloromethane. This primary emulsion (W/O) was homogenized using the Sonic Ruptor 400 (Omni International,) ultrasonic homogenizer at a power output of 40 % in the pulse mode (80%) for 3 minutes. This water/oil emulsion was immediately transferred to a beaker containing 300 ml of 0.1% (w/v) polyvinyl alcohol on a stir plate at 450 rpm for 4 hours. The microspheres were filtered between two sieves of mesh size 140 (100 microns) and 40 (425 microns) and washed five times with distilled water. Aliquots of the sample for scanning electron microscopy were then lyophilized (FreeZone® 4.5 ©Labconco freeze dry system) for 3 days [25].

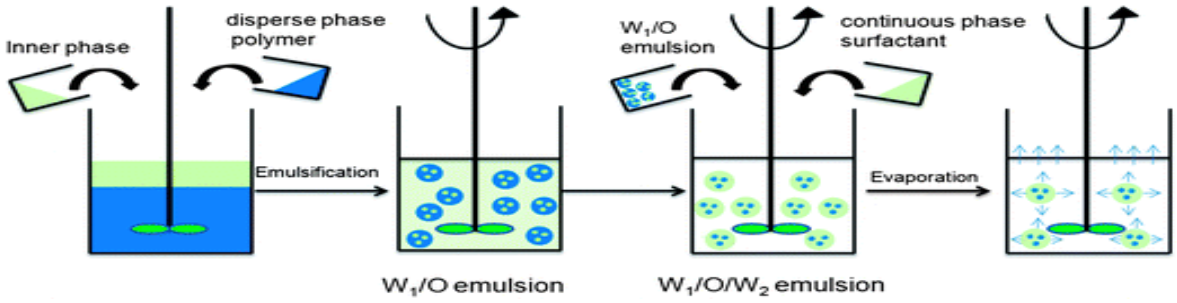

**Figure 3.1: Illustration of double emulsion solvent evaporation method [26]**

Nine more sets of microspheres with varying process parameters were fabricated to identify the effects of each variable and for the optimization of the process to obtain microspheres with the desires diameter, pore size and porosity as shown in Table 3.1:

**Table 3.1: Variation of process variables**

| Fabrication condition number | Organic solvent (DCM) volume | Amount of polymer | Amount of porogen ($NH_4HCO_{3)}$ | Aqueous solvent volume | Stir rate (rpm) |
|---|---|---|---|---|---|
| 1 | 8 ml | 500 mg | 500 mg | 2.5 ml | 450 rpm |
| 2 | 8 ml | 500 mg | 600 mg | 2.5 ml | 450 rpm |
| 3 | 8 ml | 500 mg | 600 mg | 3.5 ml | 450 rpm |
| 4 | 8 ml | 500 mg | 840 mg | 3.5 ml | 450 rpm |
| 5 | 8 ml | 400 mg | 600 mg | 2.5 ml | 450 rpm |
| 6 | 8 ml | 600 mg | 600 mg | 2.5 ml | 450 rpm |
| 7 | 7 ml | 500 mg | 600 mg | 3.5 ml | 450 rpm |
| 8 | 8 ml | 500 mg | 600 mg | 2.5 ml | 300 rpm |
| 9 | 8 ml | 500 mg | 600 mg | 2.5 ml | 600 rpm |

### 3.2.2 Scanning electron microscopy

Field emission scanning electron microscopy was used to observe the microsphere's surface morphology, diameter and pore sizes. Lyophilized samples were fixed onto an aluminum SEM stage using double sided carbon tape and sputter coated with platinum at 15 milliamps current with Hummer 6.2 Platinum sputtering system for approximately 2 minutes. Using the microscope S 3400N (Hitachi, AMRL-Clemson University), preliminary images were taken with an accelerating voltage of 10.0 kV. Once the parameters had been optimized the final high resolution images at 60x, 180x and 300x magnification were taken using SU 6600 (Hitachi, AMRL) with an accelerating voltage of 10.0 kV and a 10 mm working distance.

### 3.2.3 Preparation of uniform microsphere suspensions

The uniformity of the suspension of porous polymeric microspheres was assessed under various conditions. First, a batch of microspheres fabricated by the double emulsion solvent evaporation method were freeze dried and then aliquots of 12 and 18 mg were weighed out in 1.5 ml microcentrifuge tubes. The particles were then suspended in 1 ml of 1X PBS and vortexed for 2-3 minutes. The microspheres were then suspended in 1 ml of 1X PBS without freeze drying. This was followed by making a 1 ml suspension of the microspheres was made along with 0.36% hyaluronic acid in 1X PBS and left on the vortex at speed 8 overnight. Finally, freeze dried microspheres were treated with ethanol for 30 minutes and suspended in 1 ml of 1X PBS followed by vortexing.

### 3.3 Hydrogel preparation

The next phase of our study involved the preparation of a semi interpenetrating polymer network made from a PEG diacrylate macromer blend of PEG-bis-(AA), PEG-bis-(AP) and PEG-bis-(AB) (12.5%:37.5%:50%) with hyarulonic acid and varying concentrations of the polymer microparticles (0, 12 & 18 mg/ml). These gels were then mechanically characterized using tensile tests and their gel swelling behavior was observed by calculating gel and equilibrium water content.

#### 3.3.1 Preparation of degradable, crosslinkable PEG diacrylate macromers

A previously described semi-IPN composed of a PEGDA macromere blend of PEG-bis-(acryloyloxy aceteate), PEG-bis-(acryloyloxy proponoate) and PEG-bis-(acryloyloxy butyrate) with hyarulonic acid, that supports 3D cell spreading/migration was selected as a model gel for these studies [10] [27] [28]. Through varying the alkyl content of the chemical intermediary, hydrogels with varying degradation rates were shown to be formed.

PEGDA macromers with degradable ester bonds were made using a two-step reaction as shown in Fig 3.2:

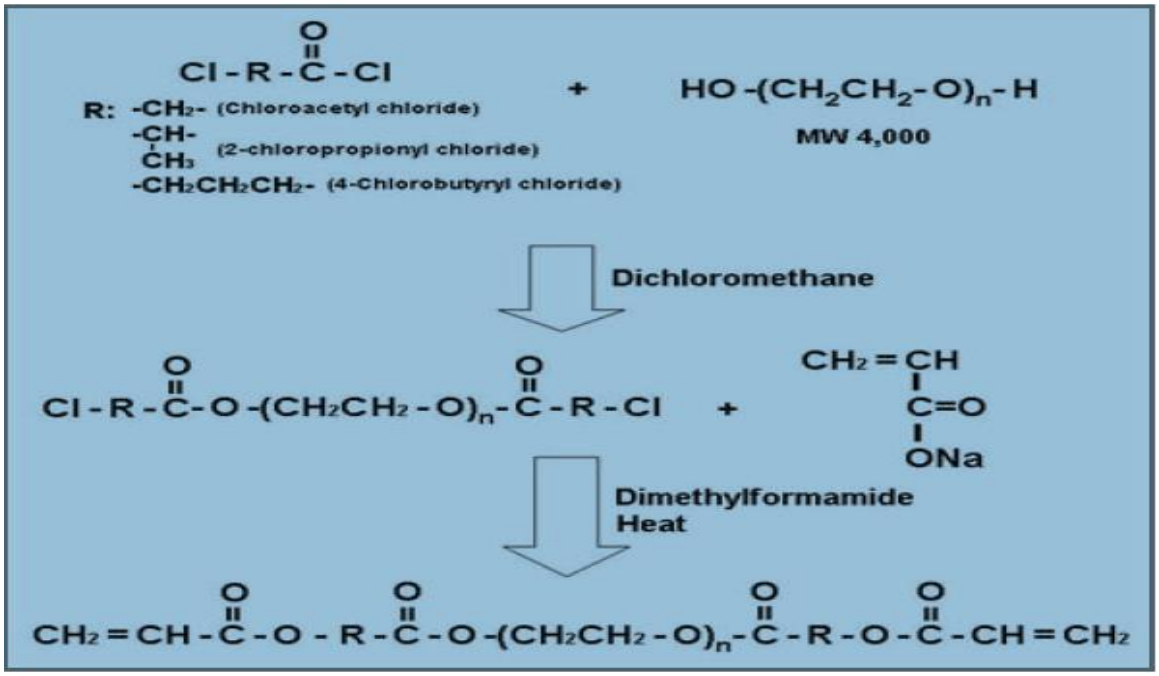


**Figure 3.2: Preparation of degradable PEG-bis-acrylate macromers [29] [30]**

PEG-bis-(AA) and PEG-bis-(AB) were provided by Dr. Ho-Joon Lee who synthesized them previously, while PEG-bis-(AP) was synthesized as follows.

### 3.3.2 Synthesis of PEG-bis-(acryloyloxy propanoate)

All glassware was cleaned in a NaOH/Ethanol (500g in 5L) and dried in a vacuum oven overnight. PEG-bis-(acryloyloxy propanoate) was prepared by reacting the terminal hydroxyl groups on PEG with (2-chloropropinoyl chloride). 15 grams of PEG (MW 3934g) was dissolved in 120 ml of dichloromethane dehydrated using calcium hydride. The amount of 2-chloropropinoyl chloride and triethylamine (TEA) to be added to the reaction solution were calculated using the formulae:

$$\text{Volume of 2-CP} = \frac{(\text{the weight of PEG} / \text{MW of PEG}) * \text{MW of 2-CP}}{\text{Density of 2-CP}}$$

$$\text{Volume of TEA} = \frac{1.8*(\text{the weight of PEG}/\text{ MW of PEG}) * \text{MW of TEA}}{\text{Density of TEA}}$$

TEA was then added to the reaction flask which was cooled on an ice bath. 2-chloroproionyl chloride was then dissolved to 30ml of dehydrated dichloromethane and added dropwise with an addition funnel to the reaction flask over 2 hours. The ice bath was then removed and the reaction was continued at room temperature for 24 hours. The reaction mixture was filtered using a fine funnel to remove the TEA-HCl salt, and then concentrated by rotary evaporation (Buchi Rotovapor®, Switzerland). The residue was redissolved in 150 ml of dichlormethane and washed 3-4 times with 15 ml of 10% sodium bicarbonate solution until the pH of the solution was neutral. The solution was then dried using anhydrous sodium sulfate. The solution was concentrate one more time by rotary evaporation and precipitated in 200 ml ethyl ether (-20°C), and washed 3 times with cold ethyl ether. The final product of this step (Product I) was separated by filtration and stored in vacuum desiccator for 24 hours.

In the second step of this process, the product obtained in the previous step was added to a flask containing dimethylformamide (10 times amount of product I) being purged with argon continuously. Once the product had dissolved, a small amount of 4-Methoxyphenol was added and an oil bath with the reaction flask submerged in it was heated to 85°C. Sodium acrylate {(5*[(weight of product I)/ $M_w$ of product I]*$M_w$ of sodium acrylate} was then added and a condenser column is connected to the flask. This reaction was allowed to run for 30 hours. The solution was then filtered and concentrated using the rotary vacuum evaporator (Buchi V 700 vacuum pump) at 55°C and 11 mbar vacuum. The solution was then precipitated in 400 ml of ethyl ether(-20°C) and washed 3

times with cold ethyl ether. The final product PEG-bis-(acryloyloxy propanoate) was gathered by filtration and stored in the vacuum desiccator for 24 hours.

The structure of the product in both steps was determined by $_1$H-NMR (Bruker Avance-300MHz) using deuterated chloroform as a solvent and compared with the NMR results obtained for the same products by previous reports in literature [28] [29].

### 3.3.3 Hydrogel photopolymerization

A PEG diacrylate macromer blend of 12.5% PEG-bis-(AA), 37.5% PEG-bis-(AP) and 50% PEG-bis-(AB) at 30 % w/v concentration was made. From this blend a working solution of 6% w/v PEGDA solution with 0.36% HA (MW 1.50MDa), 0.1% w/v I-2959 photoinitiator and varying concentrations of the polymer microparticles (0, 12 and 18 mg/ml) in 1 X PBS (0.1M, pH 7.4) was made. This solution was pipetted between two microscopic glass slides separated by mm Teflon spacers and clamped together with clips. The slides were then placed under a low intensity UV lamp (B 100 AP of Blak-ray®, wavelength 365 nm, intensity 15mW/cm$^2$). The glass slides were separated carefully after pipetting PBS around the gel. Disc shaped gels were then cut out using a hole punch (5/6 inch).

### 3.3.4 Gel content and swelling behavior

After photopolymerization, the hydrogel discs were collected in microcentrifuge tubes and placed in the -80 freezer for 4 hours. The samples were then moved to the lyophilizer (FreeZone® 4.5 Benchtop freeze dry systems of ©Labconco) overnight and then weighed (Dw1). The discs were placed in separate scintillation vials containing 4 ml of 1 X PBS and allowed to swell at room temperature overnight. The samples were then

collected, blotted on Kimwipes to get rid of excess superficial liquid and weighed (Ww2). The samples were freeze dried overnight one more time and weighed one more time (Dw2). The gel and equilibrium water content were calculated using the formulae [29]:

Gel content (%) = (Dw2/Dw1) * 100

Equilibrium water content (%) = [(Ww2 – Dw2)/Ww2] * 100

**3.3.5 Uniaxial tensile testing**

A dog bone shaped mold with 5 mm width and 1 mm depth was designed using SolidWorks 3D printed. The PEGDA macromere blend previously specified along with varying concentrations of polymer microparticles (0, 12 and 18 mg/ml) were injected into the mold clamped between two microscopic glass slides and photopolymerized under a low intensity UV lamp (B 100 AP of Blak-ray®) for 5 minutes on each side like before.

The dog bone shaped gels were obtained from the mold and equilibrated in 1 X PBS overnight. The samples were subjected to tensile testing using a MTS Synergie 100 (MTS Systems Corp.) material testing system. TestWorks® 4 software was used to interpret the data. A 10N load cell was used to subject the gels to 30% strain at 10 mm/min. Each sample was tested three times to ensure slippage did not occur. The data acquisition rate was set at 500 Hz. The sample ends were covered with small pieces of Kimwipe to ensure clamping stability.

The load exerted, extension, stress, strain and elastic modulus values were displayed by the software based on the thickness, width and grip separation inputs provided by the user. However, these values might not have been completely accurate

because the lower limit for width of cross section on the MTS Synergie 100 system was 5.080 mm and there was a zero error of 0.723 N loading force. So, manual calculations were made for the values of Young's moduli as the slope of the stress strain plot at random points in the linear elastic region between 0 and 20 % strain [29].

### 3.3.6 Statistical analysis

The data obtained for mean diameters and pore sizes of baseline [25] and optimized porous microspheres, gel content, equilibrium water content and elastic moduli were compared by ANOVA [31]. The final results were presented in terms of mean ± standard deviation.

## 3.4 Cell adhesion studies

In this part of the study, preliminary tests to establish the proof of concept of our composite system were performed. In the first test rat fibroblast cells were seeded onto spin coated microscopic glass slides for 24 hrs followed by cell fixation and staining to assess cell adhesion properties of the Strataprene® material. This was followed by live staining of rat fibroblast cells seeded onto the porous polymer microsphere (24 hour duration) component of our composite to observe cell adherence and viability *in vitro*.

### 3.4.1 Cell culture

Rat fibroblast cells were obtained from rat heads dissected in our lab. The cells were cultured routinely in T – 175 cell culture flasks using DMEM F-12 50/50, 1X, with L- glutamine and 15mM HEPES with 10% (v/v) bovine growth serum and 50 U/ml penicillin and 50µg/ml streptomycin [27]. The media was changed every three days and cells were passaged upon reaching about 80 % confluence. For cell seeding purposes, the

cells were trypsinized, centrifuged, resuspended in media and counted using a hemocytometer to ascertain the concentration of cells in a 5 ml volume. Based on the cell density required, the volume required to be pipetted from our cell suspension was calculated.

### 3.4.2 Cell adhesion on spin coated glass slides

Microscopic glass slides were cut to a length of 2.5 cm using a diamond tipped glass scribe. The slides were spin coated with 5% (w/v) PLGA and 7% (w/v) Strataprene® 3534 polymer in dichloromethane solution by Dr. Guzeliya Korneva. The slides were then left in a vacuum oven for 48 hours to get rid of the DCM. Finally, these slides were placed in 6 well plates and sterilized under ethylene oxide for 24 hours. These glass slides were prepared with the help and on facilities supported by NIGMS of the National Institutes of Health under award number 5P20GM103444-07

The spin coated glass slides were seeded with rat fibroblast cells at a density of 50,000 cells per well and cultured in media for 24 hours. The cells were fixed using 4% paraformaldehyde, permeabilized using 0.1% Triton X -100. Cells are then stained with DAPI (4,6-diamidino-2-phenylindole) which is a fluorescent dye that binds strongly to the A-T rich regions in DNA and can be used to visualize cell nuclei. This followed by cell staining with red fluorescent phalloidin dye that selectively labels F – actin in fixed cells. The cells were then observed and imaged using a fluorescence microscope.

### 3.4.3 Cell seeding experiment

The microspheres fabricated using the double emulsion solvent evaporation method were suspended in sterile deionized water and centrifuged 4 times at 4000 rpm

for 5 mins. The particles were then sterilized under UV light in a petri dish under the cell culture hood overnight.

The sterilized porous Strataprene® polymer microspheres were transferred to a 24 well plate and seeded with rat fibroblast cells in media for 24 hours in the incubator. A live Fluorescein diacetate stain was performed to observe cell viability and adhesion to the polymer microsphere component of our composite. Live cells take up the non-fluorescent FDA and convert it into fluorescent metabolite fluorescein. This conversion is esterase dependent and thus serves as an indicator of cell viability [32] [33] [34]. The cells were observed and imaged under a fluorescence microscope.

# CHAPTER FOUR

# RESULTS AND DISCUSSION

## 4.1 Double emulsion solvent evaporation

The first stage of this study involved the use of a double emulsion solvent evaporation method for the fabrication of porous Strataprene® 3534 polymer microspheres. This process has a lot of variables which affect the microsphere diameter, pore sizes and porosity in a multitude of ways. The long term goal of this study is to be able to inject these microspheres *in vivo* through 18 gauge needles to achieve cell therapy. For this application the microspheres would need to have both micro (< 50µm) and macroporosity (>50µm). As mentioned earlier, the ideal pore size for a scaffold is 3 – 5 times the size of the cells seeded on them. So, for efficient injectability and cell seeding, the microspheres would have to be in the 300 – 450 micrometer range with a pore size in the 30 – 70 µm range (Since, most mammalian cells are in the 10 – 25 µm range) [8]. The microspheres must also have an open interconnected porosity to support cell migration into the scaffold along with ECM infiltration and tissue ingrowth. A number of batches with varied parameters were then fabricated and characterized until the microsphere features were deemed optimal for our application.

### 4.1.1 Optimization of process variables

For the first baseline fabrication batch, we used PLGA instead of Strataprene® so as to eliminate the variability due to polymer when comparing with microsphere SEM images from literature [25] [35] [36] [37]. The parameters used were based on work done on macroporous PLGA microspheres by Kang et. al (2007) [25]. The microspheres were

fabricated by the double emsulsion solvent evaporation method previously described using 500 mg of PLGA dissolved in 8 ml of methylene chloride and 500 mg of porogen in 2.5 ml DI. These baseline microspheres were then washed, freeze dried and characterized using scanning electron microscopy.

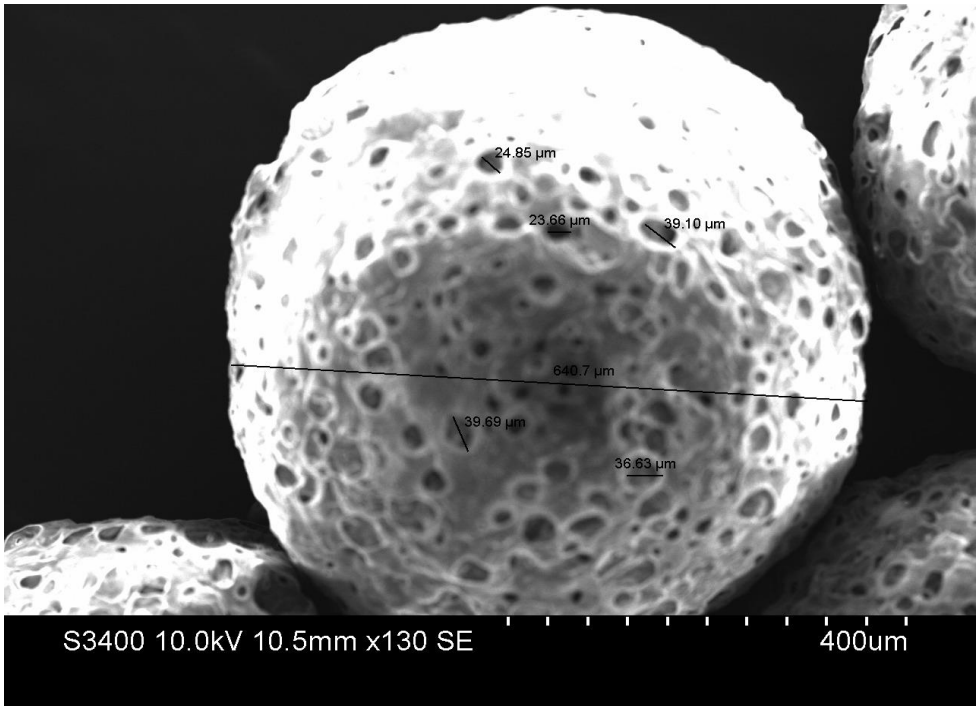


**Figure 4.1: Baseline porous PLGA polymer microspheres (500 mg of PLGA in 8 ml of DCM and 600 mg of porogen in 2.5 ml DI water at a stir rate of 450 rpm)**

The microspheres obtained with these set of conditions were mostly in the 300 – 450 µm range, which is an appropriate range for injectability through an 18 gauge needle. The pore sizes for the baseline batch however were in 20 – 40 µm range. There wasn't any macroporosity (> 50 µm) to support tissue ingrowth. Also, most of the porosity appeared to be present superficially on the surface. There didn't appear to be much pore interconnectivity either.

Based on a literature study [38] [39] [40] performed to identify the effects of process variables, we isolated stir rate, polymer concentration, porogen concentration, solvent volume of inner aqueous phase and of organic solvent phase as key factors affecting microsphere diameter, pore size and porosity.

Nine more sets of microspheres with variations in process variables as demonstrated in table 3.1 were made.

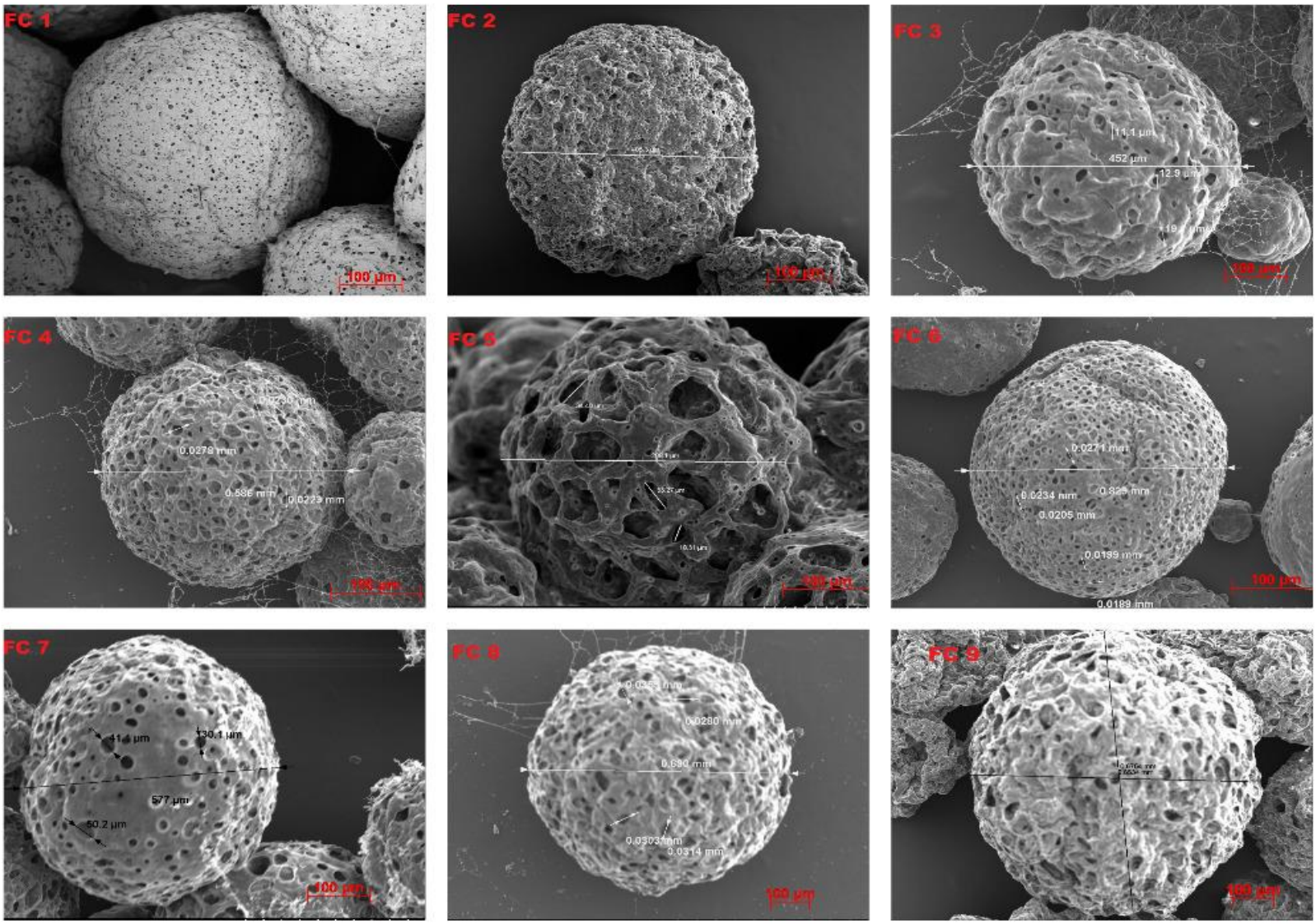

**Figure 4.2: Montage of sets of microsphere with varied fabrication conditions, from top left corner to bottom right corner; FC 1 to FC 9**

**Scale bar: 100 um**

The microspheres made with the parameters described by Table 3.1 were freeze dried and characterized by SEM.

Microspheres from fabrication condition 1 used the baseline parameters obtained from literature [8] to fabricate porous Strataprene® microspheres. The microspheres obtained in this case were mostly in the 300 – 450 μm range, but their pore sizes were in the 12 – 28 μm range. The microspheres also didn't possess an open porous structure as most of the pores were present the surface. There wasn't any macroporosity (> 50 μm) to support tissue ingrowth either.

For FC 2 the only change was increasing the concentration of porogen. The microspheres in this case showed on average larger pore sizes than the baseline batch. However, the porosity was still limited to the surface and macroporosity could not be observed either. In, the next fabrication (FC 3) we increased the porogen solvent (deionized water) from 2.5 ml – 3.5 ml while maintaining the amount of porogen at 600mg. In this case greater numbers of pores were observed although there wasn't any significant difference in the average pore sizes or any macroporosity. For FC 4, the volume of DI water was maintained at 3.5 ml, while increasing the amount of porogen from 600 to 840 mg. There was a slight increase in the porosity and average pore size in this scenario. However, these microspheres did not exhibit any macroporosity.

For fabrication FC 5, the polymer concentration was reduced from 500 mg to 400 mg in 8 ml of dichloromethane and 600 mg of porogen was dissolved in 2.5 ml of deionized water. In this case, the microspheres exhibited much larger pore sizes in the 30 – 65 µm range with adequate macroporosity. The microsphere diameters were also in the desired range of 300 – 400 µm. These microspheres demonstrated an open interconnected structure with micro and macroporosity and were considered to be the batch most suitable for our application. These microspheres were designated as the final batch with the optimized parameters.

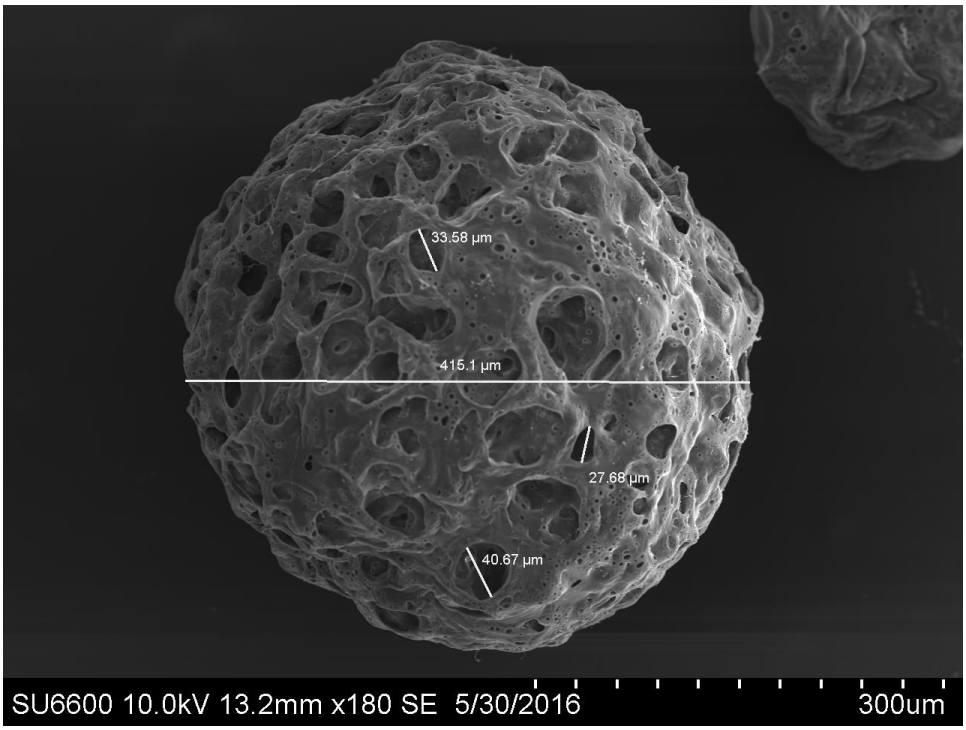


**Figure 4.3: FC 5 Stratprene® microspheres (400 mg of Strataprene® in 8 ml of DCM and 600 mg of porogen in 2.5 ml DI water at a stir rate of 450 rpm) with optimized parameters**

For FC 6, we increased the polymer concentration from 500 mg to 600 mg in 8 ml of dichloromethane. The remaining parameters were the same as batch 5. Increasing, the polymer concentration led to a drastic decrease in average pore size. There also seemed to be an increase in average diameter of the microspheres in this case. For fabrication condition 7, we decreased the organic solvent volume from 8 ml to 7 ml while increasing the volume of deionized water from 2.5 to 3.5 ml. The amount of polymer and porogen in this case were 500 mg and 600 mg respectively. The microspheres in this case didn't have any macroporosity. The microspheres in this batch generally seemed to have slightly larger pore size and diameter when compared to FC 3. For FC 8, we reduced the stir rate from 450 rpm to 300 rpm. All the other parameters were kept the same as FC 2. The microspheres in this case had larger diameters on average with a few microspheres being as large as 700 µm. The pore sizes also seemed slightly larger than the other batches with 500 mg of polymer. The porosity was still limited to the surface however and there was an absence of macroporosity. For fabrication of FC 9, we increased the stir rate to 600 rpm while keeping all other parameters the same as FC 8. The microspheres were significantly smaller and had pore sizes mostly in the 8 – 24 µm range.

Based on the observations made above from the different microsphere batches it was inferred that microsphere diameter is affected primarily by stir rate and to a lesser extent polymer concentration. Similarly, the pore size was characterized to have been affected most by porogen concentration, stir rate and to a lesser extent the volume of deionized water. Macroporosity and pore interconnectivity seemed to be most affected by polymer concentration.

### 4.1.2 Statistical analysis of baseline and optimized Strataprene® microspheres

SEM images of FC 1 and FC 5 were used to calculate the mean diameters and pore size for the baseline and optimized microspheres. The microsphere diameter for both batches seemed to be in the same range. There was a significant difference in the average diameters of the two batches however with the mean diameter of the optimized Strataprene® microspheres being more than twice that of the baseline batch.

**Table 4.1: Pore sizes and Diameters of baseline and optimized microspheres**

| | Baseline (FC 1) | Optimized (FC 5) |
|---|---|---|
| Microsphere diameter | 355.93 ± 48.10 | 353. 47 ± 50.84 |
| Pore size | 21.73 ± 8.67[a] | 44.39 ± 18.98[a] |

[a] represents a significant difference between two microsphere fabrication conditions

### 4.1.3 Preparation of uniform microsphere suspensions

Freeze dried microspheres suspended in 1 ml of 1X PBS would float to the top and form aggregates that would not go into suspension following vigorous vortexing (Vortex Genie-2, Scientific industries)

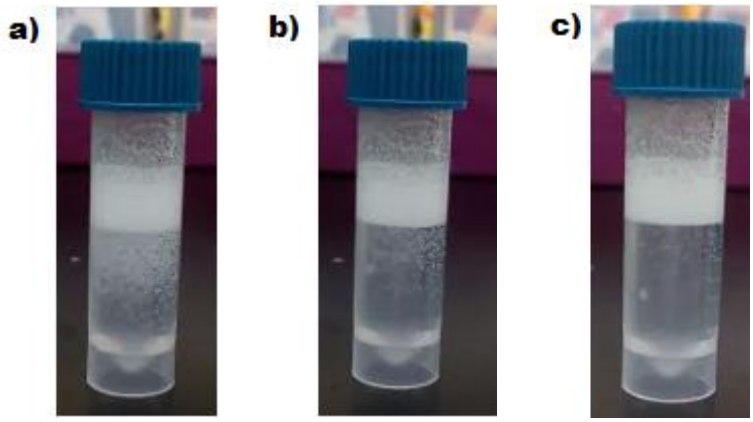


**Figure 4.4: Freeze dried Strataprene® microspheres (FC 5) in 1X PBS a) 5, b) 10 and c) 20 seconds after vortexing**.

Non freeze dried microspheres suspended in 1 ml of 1X PBS would settle to the bottom of the tube almost instantaneously. The particles would temporarily form a uniform suspension upon vortexing but the suspension would become non uniform by the time the lid was opened to pipette out a certain volume.

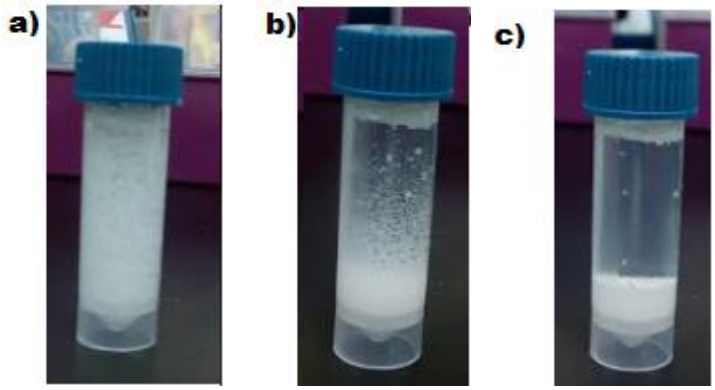


**Figure 4.5: Non-freeze dried Strataprene® microspheres (FC 5) in 1X PBS a) 5, b) 20 and c) 90 seconds after vortexing**

A 1 ml mixture of the microspheres along with 0.36% HA in 1X PBS vortexed at speed 8 overnight formed a suspension that stayed uniform for 20 minutes at a time. 100

microliters was pipetted from the suspension and freeze dried overnight. The dry weight of the microparticles was then determined based on which the concentration of microspheres in the stock suspension was estimated

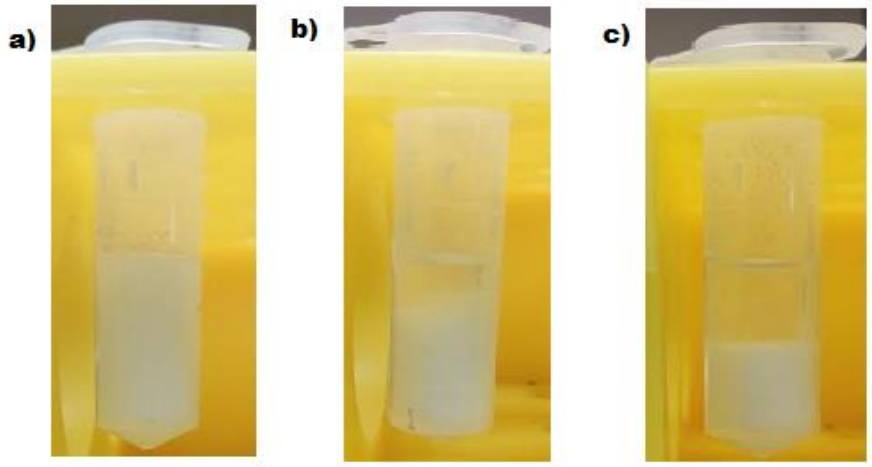


**Figure 4.6: Non-freeze dried Strataprene® microspheres (FC 5) with 0.36% HA in 1X PBS a) 1, b) 45 and 360 minutes after vortexing**

Freeze dried Strataprene® microspheres (FC 5) treated with ethanol (30 mins) and suspended in 1 ml of 1X PBS would form aggregates that would float to the top and not go into suspension following vigorous vortexing.

### 4.2.1 Synthesis and characterization of PEG-bis-(acryloyloxy propanoate)

In the first step, the PEG hydroxyl groups react with the acid chloride group on 2-chloropropionyl chloride to form ester bonds and terminal alkyl groups separated by a variable alkyl spacer. This was followed by the addition of terminal acrylate esters to the intermediate products by nucleophilic substitution reaction between the terminal alkyl chloride groups and sodium acrylate.

Following synthesis, the structure of PEG-bis-(AP) was confirmed by NMR spectroscopy. The NMR result of the PEG-bis-(AP) product was in accordance with results obtained for the same product previously synthesized by Dr. Eunhee Cho.

$_1$H-NMR peaks detected and representative spectra for PEG-bis-(acryloyloxy propanoate) using deuterated chloroform as a solvent are shown in Figure 4.7 {T= 1.65-1.75 (d, -CH3), 3.-3.7 (m, -(CH2CH2O)n-), 4.3-4.4 (t, -CCH2OC(=O)-), 4.4-4.5 (q,-OC(=O)CH(C-)Cl) ppm}.

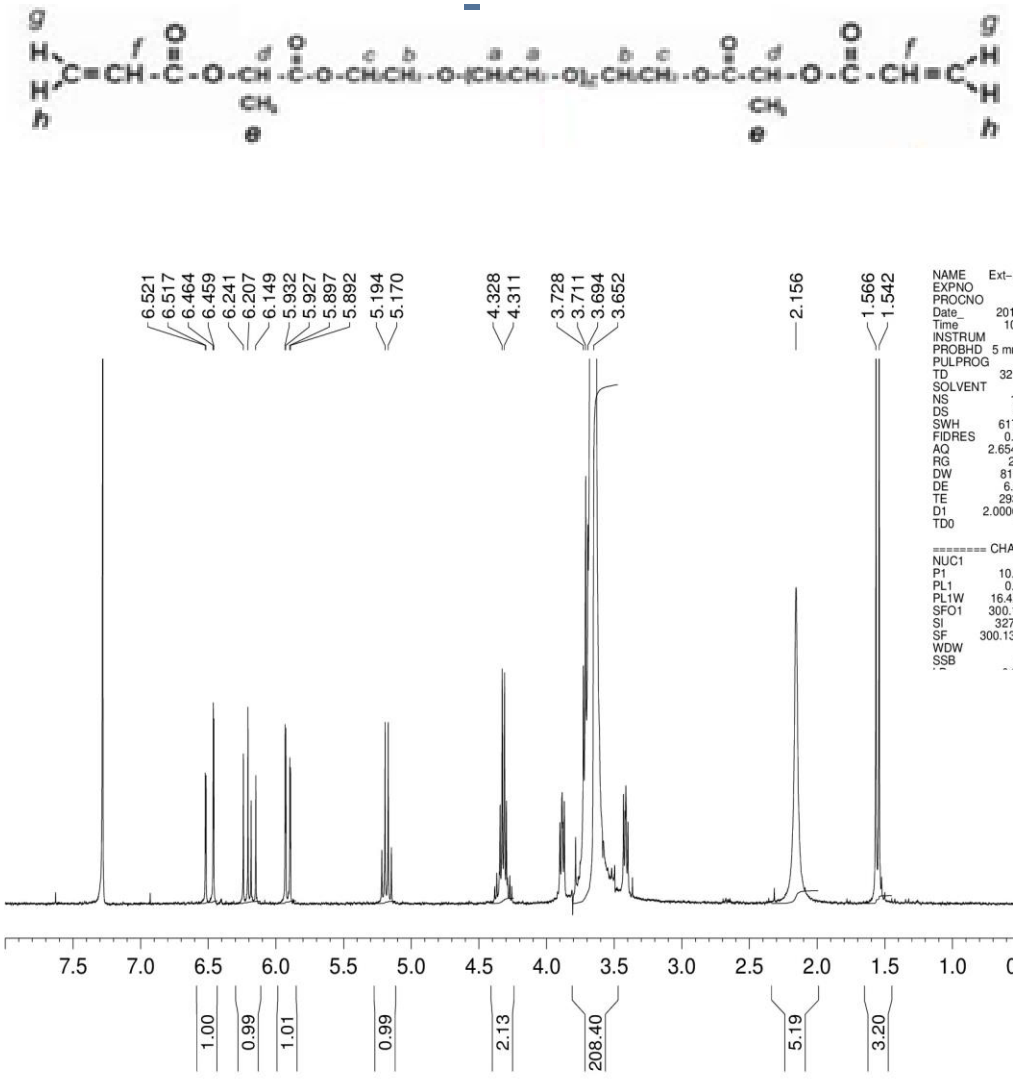

**Figure 4.7: Structure and $_1$H-NMR spectrum of PEG-bis-(acryloyloxy propanoate)**

### 4.2.2 Gel content and swelling behavior

. The gel contents and the equilibrium water contents of the different batches are shown in Table 4.3. Both gel and equilibrium water content were consistently high at different microsphere concentrations (0, 12 and 18 mg/ml). There was also a slight increase in equilibrium water content with increase in microsphere concentration. This is consistent with a slight decrease in crosslinking density due to the presence of microspheres that are not covalently incorporated in the gels. This decrease in homogeneity of the gel could also account for the decrease in gel content with increasing microsphere concentration. Overall, there was only a slight decrease in gelation efficiency with an increase in concentration of microspheres up to 18 mg/ml [29] [41].

**Table 4.2: Gelation efficiency**

| Microsphere concentration | Gel Content (%) | Equilibrium water content (%) |
|---|---|---|
| 0 mg/ml | 96.66 ± 1.15[a] | 93.31 ± 0.29[a] |
| 12 mg/ml | 92.11 ± 4.3[a] | 94.14 ± 0.27[a] |
| 18 mg/ml | 91.36 ± 2.6 | 94.46 ± 0.1 |

[a] represents a significant difference between two microsphere concentrations

### 4.2.3 Uniaxial tensile test

The mechanical properties of the gels are given below. Tensile testing showed that the elastic modulus of the gels decreased with increasing microsphere concentration. The hydrogels prepared without any microspheres were found to be the stiffest and had an elastic modulus of 47.78 ± 6.77 kPa[a]. Increasing the microsphere concentration to 12 mg/ ml led to a decrease in elastic modulus of the gels by about 12 kPa (35.68 ± 3.62 kPa[a]). Hydrogels with a microsphere concentration of 18 mg/ml showed the lowest elastic modulus (26.43 ± 2.04 kPa[a]) ([a] represents a significant difference in elastic moduli between two microsphere concentrations). This behavior was attributed to the formation of regions of stress concentration in the gel around the microspheres along with the additional mass of the microspheres being supported by the gels [42] [43].

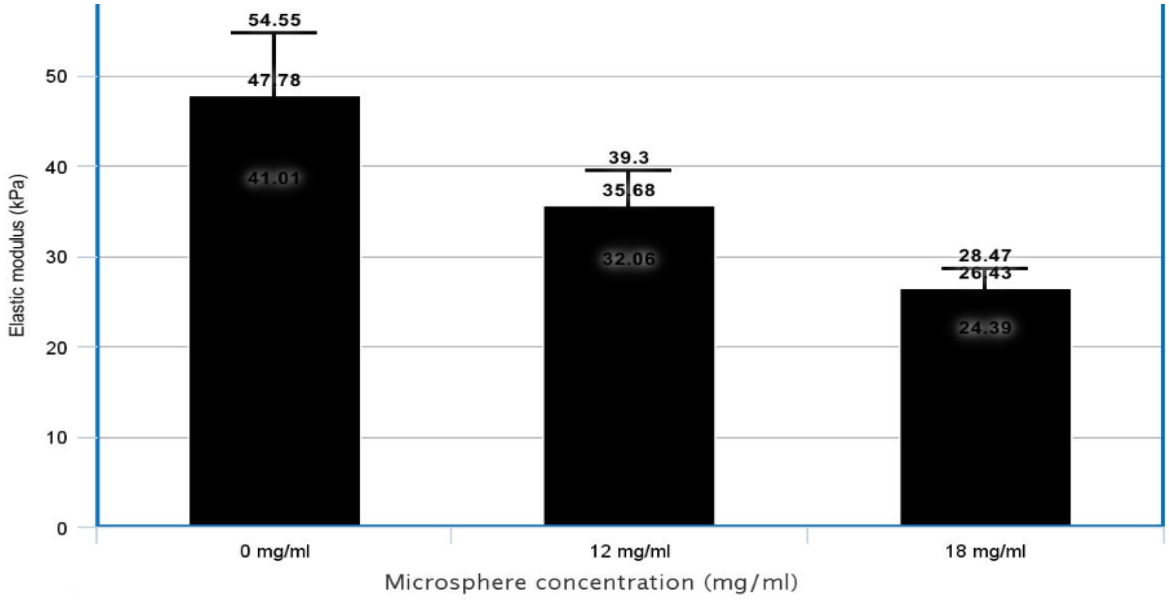

**Figure 4.8: Elastic moduli of PEGDA/HA hydrogels loaded with varying concentration of microspheres**

### 4.3.1 Cell adhesion on spin coated glass slides

Microscopic glass slides were spin coated with Strataprene® and PLGA in dichloromethane solutions. Cells were seeded at a density of 50,000 per well for a duration of 24 hours and adhesion to the Strataprene® was compared with PLGA and TCP control using DAPI and red phalloidin staining of fixed cells.

Tissue culture plastic control showed the highest degree of cell adhesion as evidenced by the high number of cell nuclei visualized using the DAPI stain. The cellular cytoskeleton also demonstrated a high degree of spreading as demonstrated by the staining of F – actin by red phalloidin.

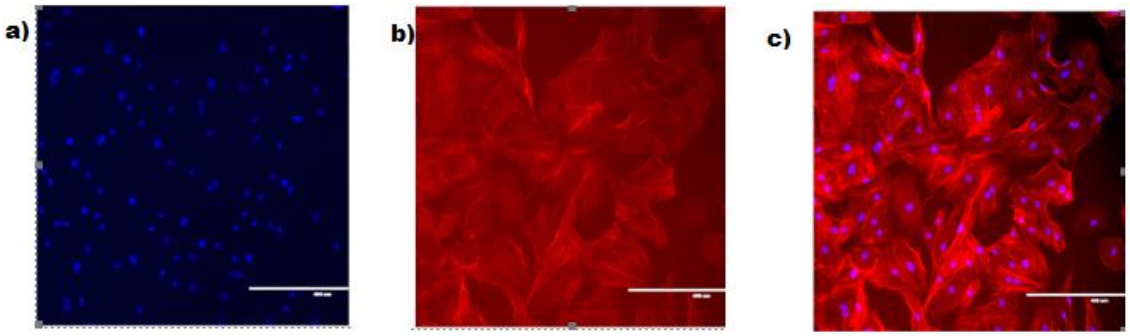


**Figure 4.9: Fluorescent images of rat fibroblasts on TCP stained with a) DAPI, b) red phalloidin and c) DAPI and red phalloidin overlayed after 24 hours of culture. Scale bar: 400 um**

PLGA coated glass slides showed a significantly lower number of cell nuclei on its surface when compared to the tissue culture plastic control. The cell morphology was

also quite different as there wasn't as much cell spreading exhibited by the rat fibroblasts cultured on TCP.

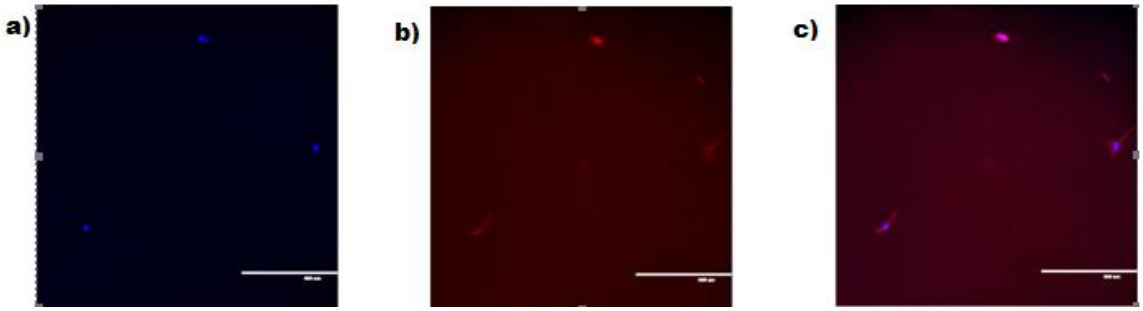


**Figure 4.10: Fluorescent images of rat fibroblasts on PLGA stained with a) DAPI, b) red phalloidin and c) DAPI and red phalloidin overlayed after 24 hours of culture. Scale bar: 400 um**

Strataprene® coated glass slides showed much better cell adhesion than PLGA. There were a greater number of cells with a more spread cytoskeletal morphology comparable to the behavior of rat fibroblasts on TCP.

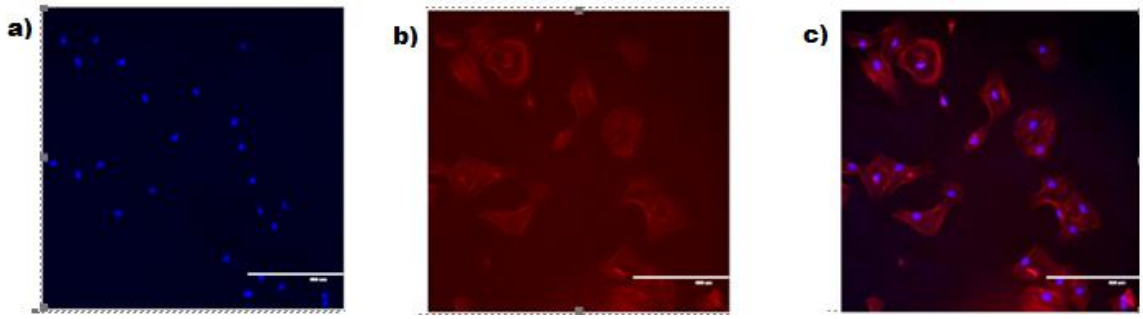


**Figure 4.11: Fluorescent images of rat fibroblasts on Strataprene® stained with a) DAPI, b) red phalloidin and c) DAPI and red phalloidin overlayed after 24 hours of culture. Scale bar: 400 um**

These studies show that cells can adhere to Strataprene® quite well without additional protein modification (e.g. coating with adhesion enhancers like fibronectin,

laminin etc). Adhesion to PLGA could be improved by fibronectin coating, but the benefit of using Strataprene® is the ability to support adhesion without this extra modification step that will either introduce animal derived proteins or human proteins that are very expensive.

### 4.3.2 Cell seeding

Porous Strataprene® microspheres were seeded with rat fibroblast cells for a duration of 24 hours followed by live fluorescein diacetate staining. There appeared to be some cell attachment when the microspheres were transferred to a fresh well (Fig 4.9) without any cells. However, cell attachment wasn't as decisive as we'd hoped for. It was hypothesized that this could be due to the presence of polyvinyl alcohol entrapped by the microspheres during emulsion stabilization interfering with cell adhesion.

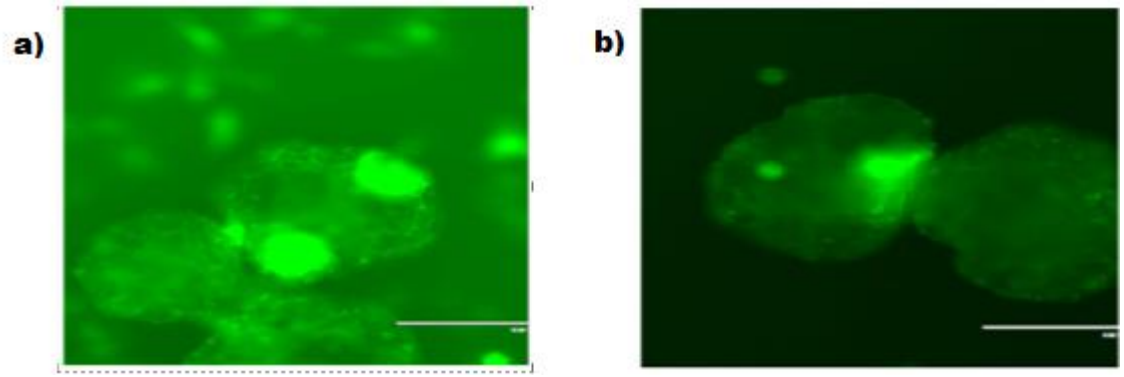


**Figure 4.12: Fluorescent images of rat fibroblasts on Strataprene® microspheres in a) the same well they were seeded in b) after being transferred to separate wells. Scale bar: 400 um**

# CHAPTER FIVE

# CONCLUSIONS AND FUTURE STUDIES

## 5.1 CONCLUSIONS

The goal of this project was to develop and characterize a novel porous polymer microsphere – hydrogel composite for tissue engineering based on cell therapy approaches. A novel polymer Strataprene® 3534 synthesized by Poly-Med, Inc. was chosen for the fabrication of porous polymer microspheres by double emulsion solvent evaporation due to its suitability for the cell scaffold application. Different batches with variations in process parameters were made in an attempt to obtain microspheres with diameters in the 300 – 450 μm range along with pore sizes in the 30 – 70 μm range. This was achieved by reducing polymer and increasing porogen (ammonium bicarbonate) concentrations. The uniformity of suspensions of both freeze dried and non-freeze dried microspheres in a 1X PBS solution and solution of PBS containing HA were evaluated. It was found that suspensions of non-freeze dried microspheres in a solution of 1X PBS containing 0.36% HA stayed uniform for 20 minutes at a time.

A Polyethylene glycol diacrylate (PEGDA) macromere blend of PEG-bis-(acryloyloxy aceteate), PEG-bis-(acryloyloxy propanoate) and PEG-bis-(acryloyloxy butyrate) with hyaluronic acid was selected for the formulation of the hydrogel component of our composite system due to the permission of rapid and sustained cell spreading by this semi-interpenetrating polymer network (semi-IPN) along with control over rate of hydrolytic degradation. The PEGDA/HA semi-IPN was photopolymerized along with varying concentrations of porous polymeric microspheres and then

mechanically characterized in order to assess the structural integrity of the composite. The elastic moduli and gelation efficiencies of the composites were compared with hydrogel only controls. It was found that an increase in concentration of incorporated microparticles led to a decrease in the elastic moduli of the composites. The composites maintained their structure and exhibited relatively high elastic moduli of 26.43 ± 2.04 kPa at 18mg/ml concentration. There was an increase in equilibrium water content and decrease in gel contents of the gel – microsphere composite with an increase in microsphere concentration. This behavior was attributed to a decrease in the efficiency of crosslinking and homogeneity of the network because of the presence of non-covalently incorporated microspheres.

Preliminary tests to establish the proof of concept of our composite system were performed by seeding rat fibroblast cells onto Strataprene® films and comparing adhesion properties with poly (lactide-co-glycolide) films and tissue culture plastic controls. Strataprene® exhibited cell adhesion and spreading comparable to TCP and significantly greater than the PLGA control. Cells were also able to adhere to the porous Strataprene® microsphere component of our composite without the use of enhancers such as fibronectin.

**5.2 Future Studies**

While the results of the pilot cell adhesion test on Strataprene® films were promising, cell adhesion to the porous Strataprene® microsphere component of our composite was not as efficient due to the presence of polyvinyl alcohol (PVA) used to stabilize the emulsion. Strategies such as surface chemical etching to eliminate PVA need

to be examined. Alternatively, the use of emulsion stabilizers such as gelatin, more compatible with cell adhesion needs to be investigated [44]. The cell proliferation and ECM accumulation properties of the composite system also need to be evaluated for the *in vitro* stage of the project.

# REFERENCES


[1] Internet, "Government Information on Organ and Tissue Donation and Transplantation," [Online]. Available: http://www.organdonor.gov/about/data.html. [Accessed 30 July 2016].

[2] R. Langer and J. P. Vacanti, "Tissue Engineering," *Tissue Engineering: From Lab to Clinic,* vol. 260, no. 510, pp. 920-926, 1993.

[3] D. Howard, L. D. Buttery, K. M. Shakesheff and S. J. Roberts, "Tissue engineering: strategies, stem cells and scaffolds," *Journal of Anatomy,* vol. 213, no. 1, pp. 66-72, 2008.

[4] C. V. Blitterswijk, Tissue Engineering, 2008.

[5] O. Qutachi, J. R. Vetsch, D. Gill and H. Cox, "Injectable and porous PLGA microspheres that form highly porous scaffolds at body temperature," *Acta Biomaterialia,* vol. 10, no. 12, pp. 5090-5098, 2014.

[6] A. Khademhosseini, R. Langer, J. Borenstein and a. J. Vacanti, "Microscale technologies for tissue engineering and biology," *Proceedings of the National Academy of Sciences,* vol. 103, no. 8, pp. 2480-2487, 2005.

[7] L. Wei, L. Yaqian, Z. Yang and Z. Xinyong, "Microcryogels as injectable 3-D cellular microniches for site-directed and augmented cell delivery," *Acta Biomaterialia,* vol. 10, no. 5, pp. 1864-1875, 2014.

[8] C. M. Murphy and F. J. O'Brien, "Understanding the effect of mean pore size on cell activity in collagen-glycosaminoglycan scaffolds," *Cell adhesion and Migration,* vol. 4, no. 3, pp. 377-3811, 2010.

[9] Internet, "NUS Tissue engineering programme," [Online]. Available: http://www.nuhs.edu.sg/research/programmatic-research/som-registered-programmes/nus-tissue-engineering-programme.html. [Accessed 30 July 2016].

[10] H.-J. Lee, A. Sen, S. Bae, J. S. Lee and K. Webb, "Poly(ethylene glycol) diacrylate/hyaluronic acid semi-interpenetrating network compositions for 3-D cell spreading and migration," *Acta Biomaterialia,* vol. 14, pp. 43-52, 2015.

[11] T. Yeung and P. C. Georges, "Effects of Substrate Stiffness on Cell Morphology, Cytoskeletal Structure, and Adhesion," *Cell Motility and the Cytoskeleton,* vol. 60, no. 1, pp. 24-34, 2005.

[12] R. G. Wells, "The Role of Matrix Stiffness in Regulating Cell Behavior," *Hepatology,* vol. 47, no. 4, pp. 1394-1400, 2008.

[13] J. Y. Wong, J. B. Leach and X. Q. Brown, "Balance of chemistry, topography, and mechanics at the cell–biomaterial interface: Issues and challenges for assessing the role of substrate mechanics on cell response," *Surface Science,* vol. 570, no. 1-2, pp. 119-133, 2004.

[14] D. Discher, "Tissue cells feel and respond to the stiffness of their substrate," *Science,* vol. 310, pp. 1139-143, 2005.

[15] M. Shoulders and R. Raines, "Collagen Structure and Stability," *Annu Rev Biochem,* vol. 78, pp. 929-958, 2010.

[16] F. Rosso, A. Giordano and M. Barbarisi, "From Cell–ECM Interactions to Tissue Engineering," *Journal of cellular physiology,* vol. 199, no. 2, pp. 174-180, 2004.

[17] J. Norman, J. Collins and S. Sharma, "Microstructures in 3D Biological Gels Affect Cell Proliferation," *Tissue Engineering,* vol. 14, no. 3, pp. 379-390, 2008.

[18] A. Atala, Foundations of Regenerative Medicine, 2010.

[19] C. Jacobs, H. Huang and R. Kwon, Introduction to cell mechanics and mechanobiology, 2013.

[20] B. Alberts and J. L. Alexander Johnson, Molecular Biology of the Cell, 2002.

[21] D. Gospodarowicz, D. Delgado and I. Vlodavsky, "Permissive effect of the extracellular matrix on cell proliferation in vitro," *Cell Biology,* vol. 77, no. 7, pp. 4094-4098, 1988.

[22] H. Du, P. Chandaroy and S. W. Hui, "Grafted poly- ethylene glycol on lipid surfaces inhibits protein adsorption and cell adhesion," *Biochimica et Biophysica Acta (BBA) – Biomembranes,* vol. 1326, no. 2, pp. 236-248, 1997.

[23] R. Michel, S. Pasche, M. Textor and D. G. Castner, "Influence of PEG Architecture on Protein Adsorption and Conformation," *Langmuir,* vol. 21, no. 26, pp. 12327-12332, 2005.

[24] Internet, "PEG or dextran surfaces," [Online]. Available: http://www.proteinslides.com/PEG-brush. [Accessed 30 July 2016].

[25] S.-W. Kang, W.-G. La and B.-S. Kim, "OpenMacroporous Poly(lactic-co-glycolic Acid) Microspheres as an Injectable Scaffold for Cartilage Tissue Engineering," *Journal of Biomaterials Science,* vol. 20, no. 3, pp. 399-409, 2009.

[26] J.-B. Fan, C. Huang, L. Jiang and S. Wang, "Nanoporous microspheres from controllable synthesis to healthcare applications," *Journal of Materials Chemistry B,* vol. 1, no. 17, pp. 2222-2235, 2013.

[27] J. K. Kutty and K. Webb, " Mechanomimetic Hydrogels for Vocal Fold Lamina Propria Regeneration," *Journal of biomaterials science: Polymer edition,* vol. 20, no. 5-6, pp. 737-756, 2009.

[28] E. Cho, J. K. Kutty, K. Datar, J. S. Lee, N. R. Vyavahare and K. Webb, "A novel synthetic route for the preparation of hydrolytically degradable synthetic hydrogel," *Journal of Biomedical Materials Research - Part A,* vol. 90, no. 4, pp. 1073-1082, 2009.

[29] E. Cho, "Hydrogel Compositions For Nonviral Gene Delivery," 2009.

[30] N. R. Vyavahare, M. G. Kulkarni and R. A. Mashelkar, "Matrix systems for zero-order release: facile erosion of crosslinked hydrogels," *Polymer,,* vol. 33, no. 3, pp. 583-599, 1992.

[31] Internet, "Analysis of variance," [Online]. Available: http://turner.faculty.swau.edu/mathematics/math241/materials/anova/aentry.php.

[Accessed 24 July 2016].

[32] T. J. Battin, "Assessment of fluorescein diacetate hydrolysis as a measure of total esterase activity in natural stream sediment biofilms," *Science and Total Environment,*, vol. 198, no. 1, pp. 51-60, 1997.

[33] K. H. Jones, "An Improved Method to Determine Cell Viability by Simultaneous Staining with Fluorescein Diacetate-Propidium Iodide," *The journal of histochemistry and cytochemistry*, vol. 33, no. 1, pp. 77-79, 1985.

[34] E. Afrimzon, A. Deutsch, Y. Shafran and N. Zurgil, "ntracellular esterase activity in living cells may distinguish between metastatic and tumor-free lymph nodes," *Clinical and Experimental Metastasis*, vol. 25, no. 3, pp. 213-224, 2008.

[35] Y. Cai, "Porous microsphere and its applications," *International Journal of Nanomedicine*, 2013.

[36] S. Gao, Y. Wang, X. D. G. Luo and Y. D. State, "Effect of pore diameter and cross-linking method on the immobilization efficiency of Candida rugosa lipase in SBA-15," *Bioresource Technology*, vol. 101, no. 11, pp. 3830-3837, 20110.

[37] Y. Hong, G. Changyou and Y. Shi, "Preperation of porous PLA microspheres by emulsion solvent evaporation based on solution induced phase separation," *Polymers for advanced technologies*, vol. 16, no. 1, pp. 622-627, 2005.

[38] H. Yushu and S. Venkatraman, "The Effect of Process Variables on the Morphology and Release Characteristics of Protein-Loaded PLGA Particles," *Journal of Applied Polymer Science*, vol. 101, no. 5, pp. 3053-3061, 2006.

[39] T. K. Kima, J. J. Yoona, D. S. Lee and T. G. P. , "Gas foamed open porous biodegradable polymeric microsphere," *Biomaterials*, vol. 27, no. 2, pp. 152-159, 2006.

[40] C. M. Agrawal, "Biodegradable polymeric scaffolds for musculoskeletal tissue engineering," *Progress in Chemistry*, vol. 16, no. 2, pp. 299-307, 2004.

[41] X. Lu, X. Cheng and Y. Sun, "Study on the swelling behaviour of copolymer hydrogel," *Chineese Journal of Polymer Science*, vol. 2, pp. 134-141, 1986.

[42] A. M. Wahl and R. Beeuwkes, "Stress Concentration Produced by Holes and Notches A," *Trans. Amer. Soc. Mech. Engrs*, vol. 56, pp. 617-625, 1934.

[43] Internet, "Bar graph maker," [Online]. Available: http://www.rapidtables.com/tools/bar-graph.htm. [Accessed 25 July 2016].

[44] A. Poursamar, J. Hatami, A. N. Lehner, C. L. d. Silva, F. C. Ferreira and A. Antunes, "Gelatin porous scaffolds fabricated using a modified gas foaming technique: Characterisation and cytotoxicity assessment," *Materials Science and Engineering C*, vol. 58, pp. 63-70, 2015.